SELECTION OF LIGHT SOURCE AND IMPLEMENTATION OF DATA ACQUISITION SYSTEM OF AN OPTICAL EXPERIMENTAL SETUP

A THESIS SUBMITTED TO
THE GRADUATE SCHOOL OF NATURAL AND APPLIED SCIENCES OF
THE MIDDLE EAST TECHNICAL UNIVERSITY

BY

ERİNÇ REYHANİOĞLU

IN PARTIAL FULFILLEMENT OF THE REQUIREMENTS FOR THE DEGREE OF
MASTER OF SCIENCE
IN
THE DEPARTMENT OF PHYSICS

JANUARY 2004

Approval of the Graduate School of Natural and Applied Sciences

_____

Prof. Dr. Canan Özgen

Director

I certify that this thesis satisfies all the requirements as a thesis for the degree of Master of Science.

_____

Prof. Dr. Sinan Bilikmen

Head of Department

This is to certify that we have read this thesis and that in our opinion it is fully adequate, in scope and quality, as a thesis for the degree of Master of Science.

_____

Assoc. Prof. Dr. Gülay Öke

Supervisor

Examining Committee Members

Prof. Dr. Sinan Bilikmen _____

Assoc. Prof. Dr. Akif Esendemir _____

Assoc. Prof. Dr. Gülay Öke _____

Assoc. Prof. Dr. Serhat Çakır _____

Dr. Ali Alaçakır _____

ABSTRACT

SELECTION OF LIGHT SOURCE AND IMPLEMENTATION OF DATA ACQUISITION SYSTEM OF AN OPTICAL EXPERIMENTAL SETUP

Reyhanioğlu, Erinç
M.S., Department of Physics
Superviser: Assoc. Prof. Dr. Gülay Öke

January 2004, 60 pages

The construction of an optical experimental setup is the objective, to measure transmission coefficient of optical components used in plasma investigations. Thus, proper light source either with continuous or line radiation spectrum should be used. In addition, the detectors' output signal is recorded on a PC based data recorder after being digitized by an analog to digital converter card.

Keyword: spectroscopy, data acquisition, transmission coefficient

ÖZ

DENEYSEL OPTİK SİSTEM İÇİN IŞIK KAYNAĞI SEÇİMİ VE DATA TOPLAMA SİSTEMİ KURULUMU

Reyhanioğlu, Erinç
Yüksek Lisans, Fizik Bölümü
Tez Yöneticisi: Doç. Dr. Gülay Öke

Ocak 2004, 60 sayfa

Plazma deneylerinde kullanılan optik parçaların ışık geçirgenlik katsayılarının hesaplanması için, deneysel optik konfigürasyon kurulması amaçlanmaktadır. Bu nedenle, sürekli veya çizgisel spektrum veren, uygun ışık kaynağının kullanılması zorunludur. Ek olarak, detektörden gelen sinyal, analogtan dijitale dönüştürücü kart tarafından dijitalleştirildikten sonra, bilgisayar bazlı bir data kaydedicisinde depolanmaktadır.

Anahtar Kelimeler: spektroskopi, data stoklanması, geçirgenlik katsayısı

To my family and my love Selen,

ACKNOWLEDGEMENTS

I would like to thank to my advisor Assoc. Prof. Dr. Gülay Öke, for her support and encouragement.

I would like to thank to Assoc. Prof. Dr. Akif Esendemir and Dr. Ali Alaçakır for the discussions about methods and instruments we used in the experiment, and also for their help during experiments.

I would also like to express my thanks to my freinds who always motivated me for the completion of this work, especially Miss. Selen Örs who always believed in me.

At last, I would like to express my sincere thanks to my little sister Ezgi, my parents Vedat & Saniye Reyhanioğlu, for their patiance, support and for their guidance in life.

TABLE OF CONTENTS

CHAPTER 1

INTRODUCTION

Plasmas are involved in several applications from lightning purposes to energy production. In that sense, it is important to deal with the measurement of plasma parameters or analysis of plasma related optical elements. Most of diagnostics is based on optical spectroscopic methods. These methods often involve optical components such as glass windows, lenses, etc. Properties of these components can change with time. Therefore, it will be useful to form an optical system that will be used for the determination of spectral dependence of optical components, for instance their transmission coefficient. It is needed to know both relative and absolute spectral dependence since both are crucial in the investigation of different parameters.

The objective is to determine the proper light source that will be included into this optical arrangement. The wavelength range to be covered is between 450 to 800 nanometers. Source can be a thermal source having continuous spectrum or a plasma source having line spectrum. Objective includes in addition, determination of spectral dependence of the detector; implementation of data recording by use of a PC based data acquisition system and installation of an evaluation program.

The system mainly will include a light source, a spectrometer in which is situated a dispersing optical element, detector and data logger. Extra elements such as pinholes, lenses can be used if necessary. After the assembly of the parts the setup at first should be calibrated.

In the next chapters, discussion about light source and about data acquisition will follow in this order. This will conclude the composition of the setup. Obviously, the setup will be used in one application, which will be discussed considering choice of light source and data acquisition along with analysis in chapter four. At the fifth and last chapter, thesis will be concluded by reminding whole concept as in the form of an outline.

CHAPTER 2

EXAMINATION OF POSSIBLE LIGHT SOURCES

Considering our objective, we will try to decide what kind of light source would be the best option for our arrangement. As stated before, the source may be a thermal source or a plasma source.

All materials emit electromagnetic radiation, the nature of which depends on the material and its temperature. Gases or vapors of atoms at less than atmospheric pressure emit radiation at discrete wavelengths when an electric current is passed through them. Excited gases containing molecules emit spectra consisting of multiple lines very close together that comprises emission bands. Solid materials emit or radiate continuous spectra across all frequencies.

Actually a blackbody is the best option of light source, since simply a mathematical relation as a function of temperature states its emissivity. Kirchoff‘s law states that for a thermal radiator at constant temperature, and in thermal equilibrium, the emissivity (e) at any given frequency is equal to the absorptance (a) for radiation from the same direction so that e=a, where absorptance is defined as the ratio of energy absorbed by the surface to that of incident energy striking the surface. [1]

An ideal surface absorbing all the energy that strikes its surface could be termed a blackbody (no radiation is reflected or emitted, thus it appears perfectly black at all frequencies). It would also stand from Kirchoff’s law that this blackbody would also be the ideal emitter of radiation.

The emissivity (e) for any black body source is defined as the ratio of the emitted radiance (ρ) by the source to the radiance of a black body (BB) at the same temperature and frequency (wavelength). The following illustrates this:

$$\varepsilon = \frac{\rho}{\rho_{BB}} \qquad \text{Eq. 2.1}$$

The spectral radiance (ρ) is defined as the radiant power (or photon flux density) emitted per unit source area per unit solid angle (conventionally expressed in $W/m^2/sr$). [1]

Max Planck derived the principles of quantum mechanics and expressed this using the concept of light quanta as discrete energy "packets" that are transferred with energy (E) proportional to the frequency of electromagnetic radiation involved. Planck's law has become one of the most widely known concepts in physics of electromagnetic radiation.

From Planck's formula, other relationship for a black body can be calculated such as the case of the Stefann Boltzmann law. The law gives the total radiance emitted from a black body source as a function of black body temperature:

$$\rho_{BB} = \sigma \times T^4 \qquad \text{Eq.2.2}$$

where σ is the Stefann Boltzmann constant.[1]

In addition to simplicity of calculation, emissivity of a blackbody is independent of the material. However, use of blackbody may be complex. Small temperature fluctuations may cause serious change in the level of emitted radiation. Thus, instead of a blackbody, other calibrated sources are preferable.

Thermal sources, as can be understood from their name, emit radiation as a result of high temperature. The main example for this kind of source is incandescent lamps. The structure of these lamps is simple. Nevertheless, they can provide relatively high level of luminescence. Combination of their simplicity and high level of luminescence makes incandescent lamps preferable. Most common of incandescent lamps is tungsten filament lamp.

This lamp consists of a current-carrying tungsten filament enclosed in a glass or quartz envelope, the bulb. The energy dissipated by the current heats the filament to incandescence so that it becomes the light source. The filament terminals are connected to the base, by means of which electrical contact is made. Parts of lamp are illustrated on the figure below. The radiation is due to thermal electrons emitted when voltage is applied.[2]

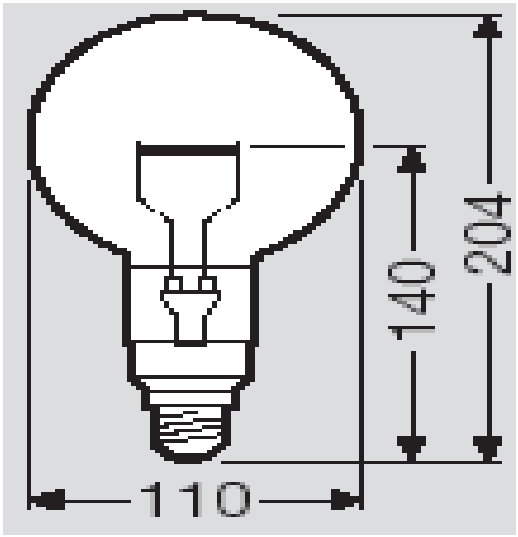

Figure 2.1: Incandescent lamp (Osram Tungsten Lamp-values in mm)

Usually the bulb is filled with gases to approximately atmospheric pressure for technical reasons. The spectrum covers wavelength range from 200 to 2400 nanometers, well satisfying the band of interest.

In comparison with the blackbody tungsten ribbon lamp has many advantages. The heating by means of an electrical current is much simpler and makes an accurate adjustment and high constancy of the radiant intensity possible. Since the ribbon filament is mounted in vacuum or in an inert gas, high temperatures can be reached easily. Another advantage of the tungsten compared to other materials is that tungsten can be obtained in high purity. In addition, cleaning the surface and shaping is much easier.

In many applications, tungsten filament lamp is used as light source since its radiant intensity as a function of temperature and wavelength is known for certain temperatures. In fact the blackbody is the only source whose intensity is described by formula, namely Stefan Boltzmann equation for blackbodies. This equation contain no parameter related to the material blackbody is constructed. Thus, a blackbody is a primary standard.

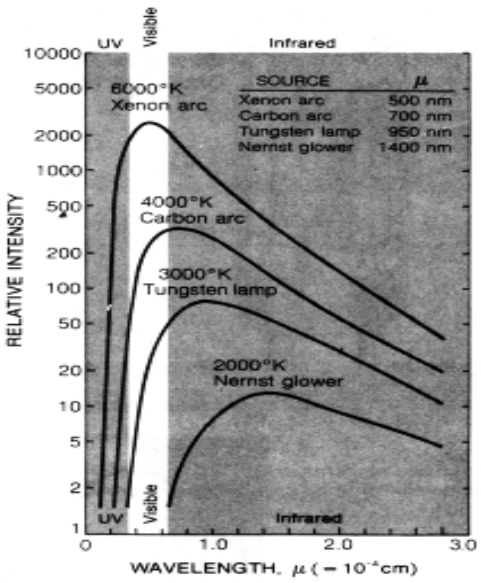

Figure 2.2: Emmission curves for several typical blackbody radiators [3]

Although the lamps listed in the figure are not total blackbodies, they are much more useful in terms of simplicity stated above, in laboratory experiments.

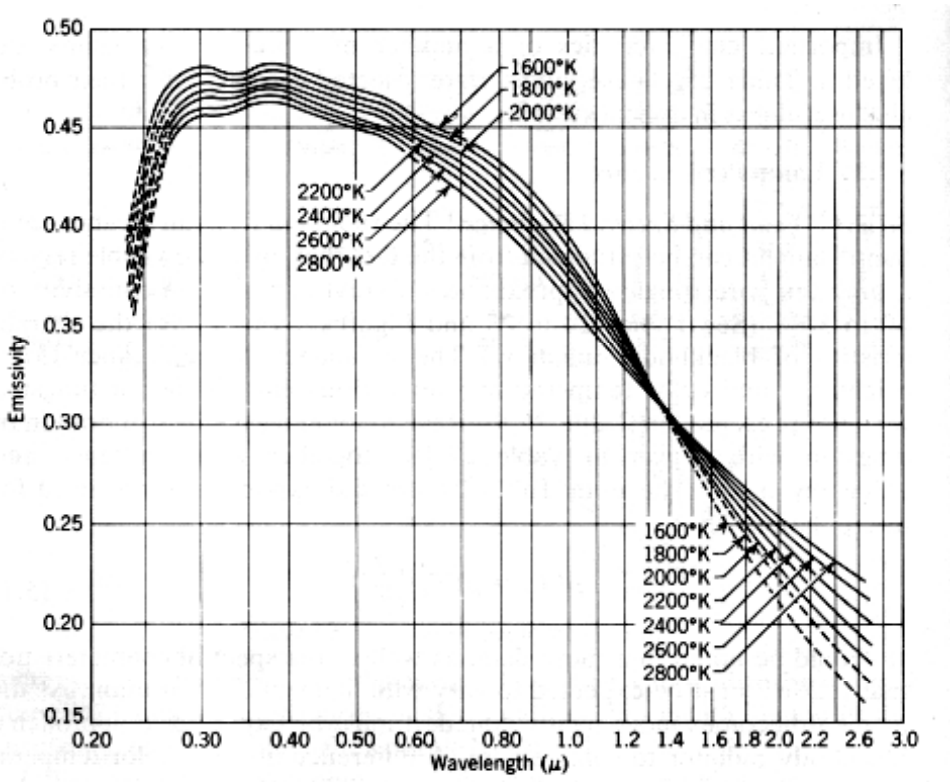

Figure 2.3: The emissivity of tungsten filament as a function of wavelength and temperature (after De Vos)[4]

With the known absolute emissivity of tungsten filament in different temperatures, a tungsten lamp can easily be added to the system as it is a primary standart source like a blackbody.

The other type of source is the one that emit radiation as a result of electric discharge through gases. Light sources based on the excitation of gases follow the incandescent lamp in importance. Specifically, incandescent lamps suffer from three major limitations, which may be overcome by the use of gaseous discharge lamps. For instance, with incandescent lamps it is not possible to get a spectrum where higher intensity is observed for a single wavelength.

The principle of discharge lamps is simple. When a moderate voltage is applied across a gas consisting of neutral atoms, these atoms will become

somewhat distorted but no visible effects will occur. If, on the other hand, free electrons are present, they will be accelerated and may cause excitation and subsequent emission of radiation by colliding with the atoms. This phenomenon forms the basis of gaseous discharge lamps.

The energy of radiation is dependent on the energy levels of the atoms in the medium. The radiation will be concentrated in discrete energies. These are related to discrete energy levels corresponding to orbits electrons have. The applied voltage causes the electrons to change their levels. Disturbed electrons move back to original position while they give out excess energy in the form of radiation. Due to uncertainty, not all radiation corresponds to one frequency but radiation is observed as a band having at the center the main energy line.

If the voltage applied across the gas is now less than the minimum excitation potential (V_1) corresponding to the energy difference between the ground state and the first unstable excited state, all but a negligible part of the collisions will be elastic and there will still be no visible effects; but when the applied voltage exceeds V_1 the collision may leave the atom in an excited state. As a rule, the atoms excited will soon return spontaneously to the ground state and will emit monochromatic radiation. The frequency of this radiation is determined in terms of Planck's constant and the applied voltage V_1, which will be as follows:

$$\omega = \frac{2\pi e V_1}{h} \qquad \text{Eq.2.3}$$

where e is charge of an electron.[1]

With increased voltage, higher states of excitation are attained and radiation at other wavelengths is emitted. When the applied voltage exceeds the

ionization potential (Vi), the atom may be ionized by the collision, which adds to the current another electron and a positive ion. These will be accelerated to the anode and cathode, respectively.

At low pressures and currents recombination of an electron with a positive ion in the gas is improbable. On the other hand, there will occur a sustained discharge, which will emit radiation not only in a single frequency, but in a range. This sustained discharge is called a glow discharge. [5]

With the use of thermal sources and discharge of gases it is possible to design very different types of light sources. Most instrumentation used to measure the region from 190 to 2500 nm utilizes a combination of the quartz Tungsten—halogen lamp for the visible and near-infrared regions (approximately 350 -2500 nm) and the DC deuterium lamp for the ultraviolet region (from 190 to 350 nm). The useful working ranges for the most common sources are:

Quartz Tungsten halogen Filament lamp	(220- 2700 nm)
DC deuterium lamp for UV	(185—375 nm)
Pulsed xenon arc lamp	(180--2500 nm)
DC arc lamp	(200-2500 nm)

As mentioned above, there are lots of lamps with different type of spectrum. Next figure gives more examples. [6]

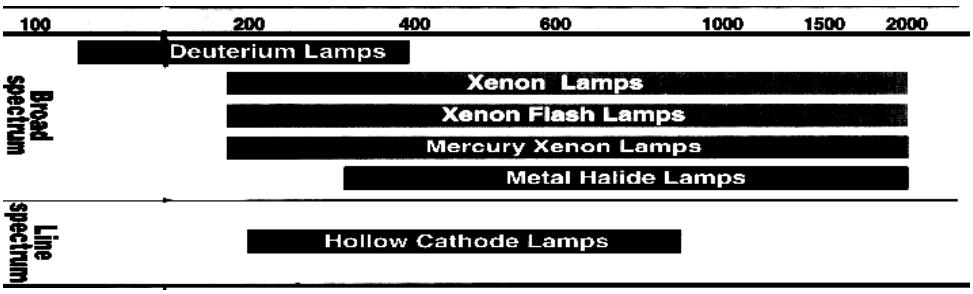

Figure 2.4: Several lamps and their wavelength ranges [7]

When selecting the light source there are several parameters to consider. The spectrum range, intensity, stability, life hours, etc… In the case of our experiment, namely measuring the transmittance of an unknown glass, not all parameters are relevant. What is sought is that spectral range to be between 450 to 1000 nanometers radiating continuously. Furthermore, since the calibration of the optical components may be required, the source has itself to be a primary standard or has to be previously calibrated with respect to one. Considering these, the best choice is to use a tungsten filament lamp at a proper temperature. Also, the use of tungsten lamp will make it possible to make absolute calibration.

In the experiment we have used Osram's Tungsten Strip Lamp. The lamp is calibrated in Institute of Plasma Physics at Juelich, Germany. The temperature of tungsten filament is known for specific current values.(Table 1). The filament dimensions are known to be 1.6x30 mm. Thus, the calculation of photon flux is possible, starting from a perfect blackbody, and using information introduced by De Vos, in 1954.

Table 2.1: Calibration values

Kelvin	Volt	Ampere
2400	7,55	13,02
2500	8,61	13,96
2600	9,68	14,87
2700	10,92	15,96

CHAPTER 3

IMPLEMENTATION OF DATA RECORDING SYSTEM

Data acquisition and storage progressed from photography of oscilloscope traces in the 1960's to use of on-line computers in the 1970's. Data acquisition in the general sense is the process of collecting information from the real world. For most engineers and scientists these data are mostly numerical and usually collected, stored, and analyzed using a computer. The use of a computer automates the data acquisition process, enabling the collection of more data in less time with fewer errors. [8]

Human observers are limited in how fast they can record readings (say. every second, at best) and how much data can be recorded before errors due to fatigue occur. An automated data acquisition system can easily record readings for very small time intervals (i.e. every millisecond), continuing for arbitrarily long time periods. In fact, it is easy to acquire too much data, which can complicate the subsequent analysis. Once the data are stored in a computer, they can be displayed graphically analyzed, or otherwise manipulated.

Most real world data are not in a form that can be directly recorded by a computer. These quantities typically include temperature, pressure, distance, velocity, mass, and energy output (such as optical, acoustic, and electrical energy). Very often these quantities are measured versus time or position. A physical quantity must first be converted to an electrical quantity (voltage, current or resistance) using a sensor or transducer. This enables the data to be

conditioned by electronic instrumentation, which operates on analog signals. The value of analog signal can change an arbitrarily small amount within an arbitrarily small time interval.

Data must be in digital form to be recorded (and understood) by computer. Digital waveforms have discrete value and have a specified constant time interval between succeeding values. This gives them a stepped appearance.

The process of converting an analog signal to a digital one is called analog to digital conversion, and the device that does this is an analog to digital converter (ADC). The resulting digital signal is in a known range (scale factor) separated by a fixed time interval (or sampling interval).

The reverse process of converting digital data to an analog signal is also possible and it is called digital to analog conversion, and the device that does this is called a digital to analog converter (DAC). Some common applications by DAC include control systems and waveform generators.

Personal computers are the inevitable part of data acquisition systems. The speed, possibility of storing a very large amount of data, and ease of use of quality graphic interfaces makes them perfect system elements. Nowadays, computers that also store data with the help of software, control all experiments.

Software is as important to data acquisition systems as hardware capabilities. Inefficient software can waste the usefulness of the perfect data acquisition hardware system. Conversely, well-written software can squeeze the maximum performance out of the well-designed hardware.

Data acquisition software controls not only the collection of data but also its analysis and eventual display. Ease of data analysis is the major reasons behind using computers for data acquisition. With the appropriate software,

computers can process the acquired data and produce outputs in the form of tables or plots. Without these capabilities, the equipment is no else than an expensive data recorder.

The physical quantities of interest to be measured using an electronic data acquisition system, must first be converted to electrical quantities. This is done by the detector in the system, namely the photodiode in our case. Since the transducer is the ‘‘front end’ of the data acquisition system, its properties are critical to the overall system performance. Some of these properties are sensitivity, stability, noise, dynamic range, and linearity. Looking at sensitivity and noise, if the transducer sensitivity is too low or its noise level too high, signal conditioning may not produce an adequate signal to noise ratio.

The noise is a limitation on the measurements. No measurements can be done certainly. There will be errors and unwanted additional signals, both internal and external, which will disturb the system, and output data. There are several types of noise. For an electronic system, three of them are worth mentioning: thermal noise, shot noise and flicker noise. [3]

Thermal noise is due to the movement of electric charges. Voltage value of thermal noise is dependent on resistance, temperature bandwidth, and independent of the frequency, meaning that it is always present. The level of thermal noise may not be seen as insignificant but, with amplification it may reach several volts, making it harder to distinguish between the signal and noise.

Shot noise is another type, resulting in due to fluctuations of charge carriers across a junction. Like thermal noise it is independent of the frequency, it is always present. Shot noise is related to DC current across junction. Limiting the current through the device is an effective way of dealing with the shot noise.

The third source is flicker noise. Main difference between the flicker

noise and the previous two is that flicker noise is frequency dependent. It is inversely proportional to frequency. The reason of this kind of noise is not well understood. Observations show that the level of flicker noise in solid-state devices is higher than its level in vacuum devices.

Even when there is no input, a transducer will measure a quantity, namely the above described noise, which is also called dark current. In the scope of the optical system related to this text, the transducer used is Hamamatsu S2506-02 Si PIN Photodiode. The maximum dark current, is given as 10 nanoamperes which is, in the output has to be measured, in the range of milivolts. The output signal of the photodiode is analog voltage. The physical quantity, intensity of incoming light, is transferred into a voltage signal. In order to record data, this signal should be converted into a digital signal. This is done by analog to digital converters.

3.1. Analog to Digital Converters PCL711S-PCL818H

As previously noted, we live in an analog world. Nearly all real world measured quantities are analog. Analog waveforms are defined as smooth continuous functions that have derivative existing nearly everywhere. On the opposite, digital quantities have discrete values that vary by steps. Digital electronics mostly uses the binary values, the true or false logic. One binary value either true or false is called a bit. It takes many bits grouped together to represent a useful quantity. In general, a collection of n bits can represent 2^n discrete levels. For example, a group of eight bits is referred to as a byte, where 2^8, 256 levels, for a representation of values in the range of 0 to 255 (or -128 to +127). Increasing the number of bits improves the digital representation of the analog signal within a given dynamic range. The concept of dynamic range is very important for data acquisition systems. By definition, the dynamic range of

a data acquisition system is the ratio of the maximum value that can be measured to the smallest value that can be resolved. This number is often represented in decibels (dB) as:

$$\text{Dynamic range (dB)} = 20 \times \log_{10} (\text{max/min}) \qquad \text{Eq.3.1}$$

As the relation shows the higher the dynamic range is, the better the resolution is. [8]

The resolution is an important parameter together with the sampling rate. They are important characteristics of an ADC, analog to digital converter. ADC resolution is defined as the smallest change that converter can detect in a measurement. This value is actually a percentage of the full scale reading. For example, a 10 bits ADC has a resolution of approximately 0.1% (1/1024). Note that an ADC's accuracy can be no better than its resolution for an individual reading. Sampling rate for an ADC is the frequency of recording data. This property becomes more important when measured quantity has a rapid rate of change. Not using a proper ADC in terms of the sampling rate, some data would definitely be missed, causing wrong interpretation of measurement. In order to be sure about not missing any data, an ADC with a sampling rate much higher than the frequency of the source should be implemented to the system.

Analog to digital converters are electronic circuits implemented into computers as hardware. These are mostly presented to the user as in the forms of plug in cards.

There are several types of ADC cards belonging to various manufacturers. Some concentrate on one application such as to input analog signals and convert them into digital form; some are willing to cover a larger range of applications, thus, includes also digital to analog conversion or timer control units on the same card.

For the control and operation of ADC cards, every manufacturer also develops software uniquely designed to match the specifications of the hardware. Parallel to the quick change in the market, there are several programs compiled to help researchers in data acquisition and automation. Usually, menu based style is preferred in order to ease the operation.

We used analog to digital converters of Advantech Co., in the form of plug in card. The PCL 818H and PCL 711 cards are connected to computer via extension bus on the main board. Installing software drivers provided together with the cards, converters are ready to operate. The 12 bit 818H card has 16 single ended channels and PCL 711 has only 8 input channels. Each channel is accessed by a pin connection. With the grounds counted, 818H has four "20 pin" access for analog input-output, digital input-output separately. Analog input port is illustrated in figure 3.1.

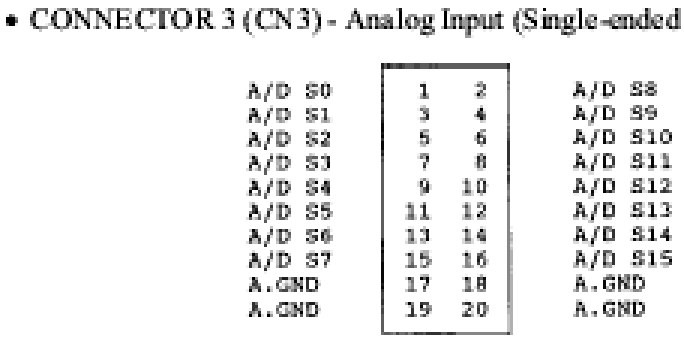

Figure 3.1: Analog input 20 pin connections for PCL818H. (A/D S #) is analog input channels (s stands for single ended), A.GND are ground pins.

The minimum value of input that can be measured is important for the system. We need to be able to measure a change of 0.01 Volts at minimum.

The sampling rate is much higher -100 KHz- than needed. Scanning less than a nanometer and recording 10 data for each second is more than enough in order to plot spectra obtained. This holds Nyquist Theorem stating that sampling frequency must be at least double of the input signals frequency. [8]

There are several switches, jumpers and variable resistors on the card.* These enable user to adjust cards properties as required. The calibration of the card is also done by changing these.

3.1.1. Calibration

Calibration of card is necessary because it should read signals accurately. The procedure is simple and involves several measurements. First of all when grounded, a channel should read zero input. With the electronic noise it will never equal zero but must be as close as possible to null.

The next step in the calibration is the adjustment of offset and maximum input levels. As going through the calibration procedure, it is observed that offset and maximum level adjustments were already in good shape. So, calibration was complete.

Analog to digital converters also have some level of noise as the photomultiplier. For an electronic system, two of the previously introduced noise contributions are worth repeating; thermal noise and shot noise.

Voltage value of thermal noise is dependent on resistance, temperature bandwidth, and independent of the frequency, meaning that it is always present. We have introduced previously that this kind of noise is very small for PCL cards. One other contributor to that is detector dark current. The level of thermal noise may not be seen as insignificant but with amplification it may reach several volts, making it harder to distinguish between the signal and noise.

* See Appendix C for switch and jumper locations

Like thermal noise, shot noise is independent of the frequency it is always present. Shot noise is related to DC current across junction. Limiting the current through the device is an effective way of dealing with the shot noise. To cope with this noise it is useful to have minimum number of junctions, or choose stable connections between cables.

3.1.2. Composition of Task and Display Screen for PCL Cards

Advantech Co. provides customer with a software program, designed for data acquisition and control application and as well an application builder for all kind of automation: "The graphical interface makes it easier to construct a task, which will control the system or which will read and record data. The software enables the user to control several tasks at the same time. VisiDAQ 3.1 task designer uses a data flow-programming model that frees operator from the linear architecture of text-based languages."*

The introduction to information file of software itself, describes very well the structure of VisiDAQ 3.1. We have constructed diagram below to control and record data.

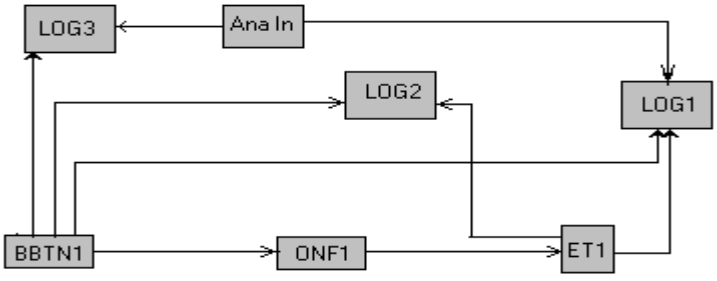

Figure 3.2: Task constructed in VisiDAQ to control data logging process.

*Part of Advantech Co. VisiDAQ 3.10 Readme File

Analog Input (AI) is the converted digital signal from PCL818H. The number of data recorded is shown with the use of timer (ET1). Since the interval and the constant speed of scan is known, this data can easily be converted to wavelengths. Assigning the start wavelength to first, end wavelength to last data recorded, intensity (in volts) versus wavelength graph can be plotted.

Data are stored in three different files (LOG1-3). Time and analog input voltage separately recorded to two files, and also they are recorded into the same file. This is done to have more options while analyzing data afterwards. The data storage does not start immediately. To start and to end data acquisition the software waits for command. (BBTN1) In addition to that, a display window is prepared for observation during the experiment. As the data are recorded, it will also be displayed on the screen.

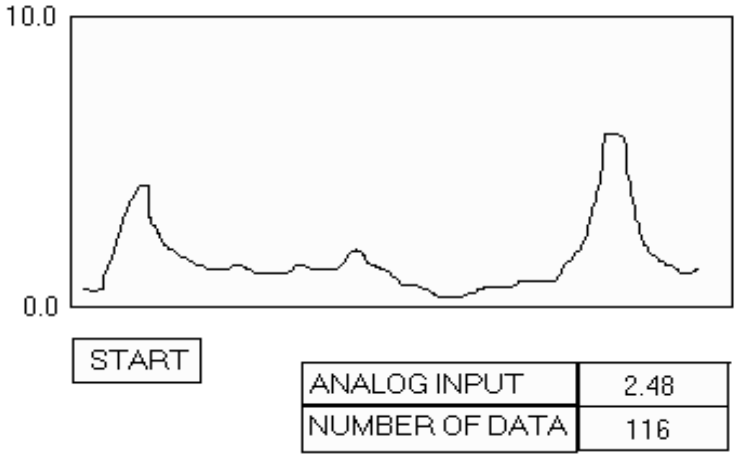

Figure 3.3: Display and control screen designed in VisiDAQ for monitoring recorded data. (The spectrum shown is imaginary)

When the task composition is run, display screen appears. Analog input value is written and plotted continuously. It is possible to see number of data recorded. The sampling rate in the experiments is chosen between 1 and 10 Hz.

CHAPTER 4

EXPERIMENTAL DATA

The aim was to construct an optical experimental setup in order to measure the transmission coefficients of optical components used in plasma applications. The setup is described above concentrating on the selection of both the light source and data acquisition system.

At the next step comes the determination of transmission coefficient of an unknown glass for specific wavelength values. Method is simple enough. We introduce the glass into the setup we have just constructed. Having measured the intensity coming from the light source both with the glass inserted and without the glass, the ratio of two measurements should give the transmission ratio of incident light.

4.1 Setup Characteristics

Considering elements of the setup, starting from the light source up to the data acquisition, there are several factors that limit the accuracy and range of data. The deposited tungsten at the surface of the light bulb, the resolution of the monochromator which is nearly 1.5 nm at full slit width, the insufficient sensitivity of ADC card that is in the range of milivolts, the lack of an instrument that can measure diode output current which is in the range of nanoamperes, the

amplification of the noise due to large resistance used is complete list of negative factors.

The diffraction and interference at the slit are neglegted since the slith width is much larger than wavelength. The temperature dependence of components, such as the PIN diode, is almost constant comparing with negative factors listed above. The efficiency of the Ebert type monochromator between 450 to 800 nm is given in different textbooks and papers to vary between 0.96 and 0.97, therefore it is also negligible. Stray light is also neglected.

The sensitivity of the system covers the range between 450 to 500 nanometers. Below 450 nm, signal to noise ratio is too small, thus recording of data is not efficient. When the diode is connected to ADC card, at a specific wavelength, the output measurement varies constantly about 2mV. However, if output is measured with other digital instruments, oscilloscope and multimeters, the variations are only equal to internal noise of these equipement. Furthermore, when there is no incident light on diode, the ADC card measures values between –300 mV and 300 mV with no definite waveform or frequency.

The output of Hamamtsu Si PIN photodiode depends on the distance of light source to enterence slit, temperature of tungsten filament of source, the value of resistance attached to it and the widths of both slits.

The elements present in the setup were calibrated Osram Tungsten Ribbon lamp, Jarrell-Ash Ebert type monochromator, Hamamatsu Si PIN photodiode and Advantech PCL711 analog to digital converter card for data acquisition. The procedure was repeated with two more diodes. Results are included at the end of thesis.

4.2 Experimental Procedure and Data

4.2.1 Aim of the procedure

The aim is to determine spectral dependence of photon flux of calibrated ligth source, then calibrate the diode in terms of its spectral sensitivity by comparison to flux of the source. With this reference one will be able to measure flux of any other source implemented on the system, or can calculate transmission coefficient of an optical component by comparing the flux measured with and without the component inserted to the system.

4.2.2 Method and Specifications

Through the system, all parts are fixed. Only the grating inside the monochromator is dynamic which can be set to different scan speeds. In the experiment the scan speed is set to 500 Angstrom per minute in order to compansate the low resolution of the monochromator. The tungsten strip is 7 centimeters away from the entrence slit. The slit width is 2 milimeters for both enterence and exit sits. The temperature of tungsten ribbon is set to 2600 and 2700 Kelvin.

The PIN photodiode can work without need to a source since it generates power due to photovoltaic effect. The leads of the diode are directly connected to ADC card, which is equivalent to a voltmeter. The output signal in Volts should be directly proportional to the photocurrent. The data recorded was between 10mV to 220mV with serious drops between 450nm-500nm. Although data seemed convenient for calculations, alternative methods had to be

implemented since serious fluctuations and inconsistencies between successive data sets has been observed

Most obvious alternative method was to construct the circuit for Si PIN photodiodes introduced in the manufacturers cathalog shown in the figure below, which allows increase in linearity and amplification of the output signal, where we choosed R=1 KΩ, V_R=12 V, C=20 nF – 100 nF and Rf a rheosta between 100Ω-100KΩ referring to values recommended by the manufacturer or by various books on electronic devices.

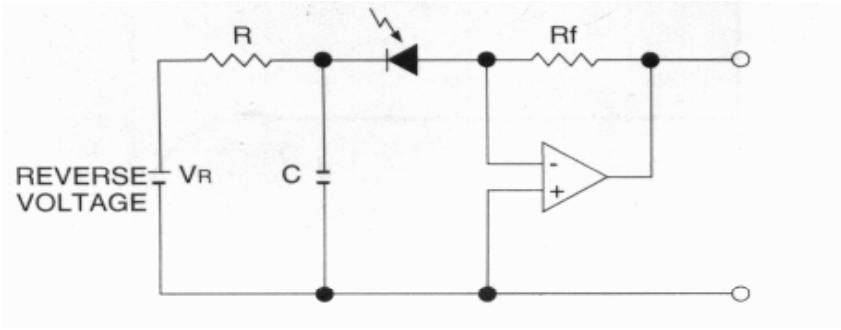

Figure 4.1: Circuit constructed as given in Hamamatsu cathalog

Data obtained was between 1mV to 25mV. The noise level and fluctuations were in the 3mV range due to the amplification, which was quite more disturbing.

The final choice was to connect a resistance in series to the leads of the diode and measure the voltage over the resistance with ADC card connected parallel to the resistance.

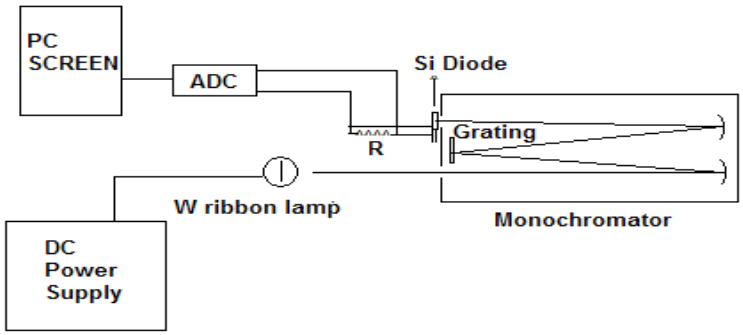

Figure 4.2: Schematic of the experimental setup

In order the outputsignal to be detectable by the ADC card and to have significant differences compared to noise between minima and maxima of the data, the resistance values have been chosen as 120 K and 265K. The data was between 20mV - 210mV and was smoother than previous tries. No sudden drops were observed and consistent noise of maximum 3 mV having excellent consistency between successive data sets. The next figures show data points recorded using S2506-02 silicon photodiode at different ribbon temperatures and different resistance values, as well as the fitted curve.

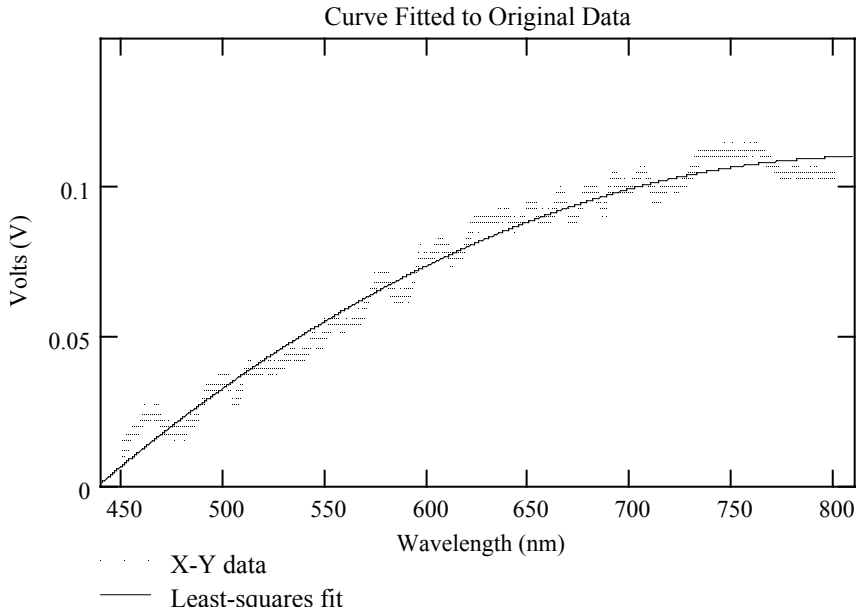

Figure 4.3: Data taken and fitted curve at 2600K with 120K resistance

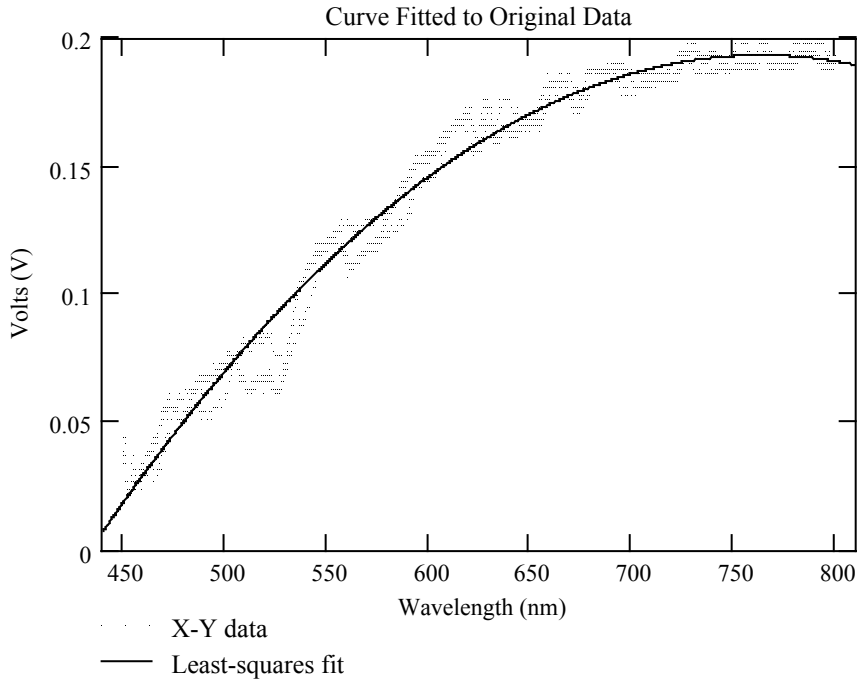

Figure 4.4: Data taken and fitted curve at 2600K with 265K resistance

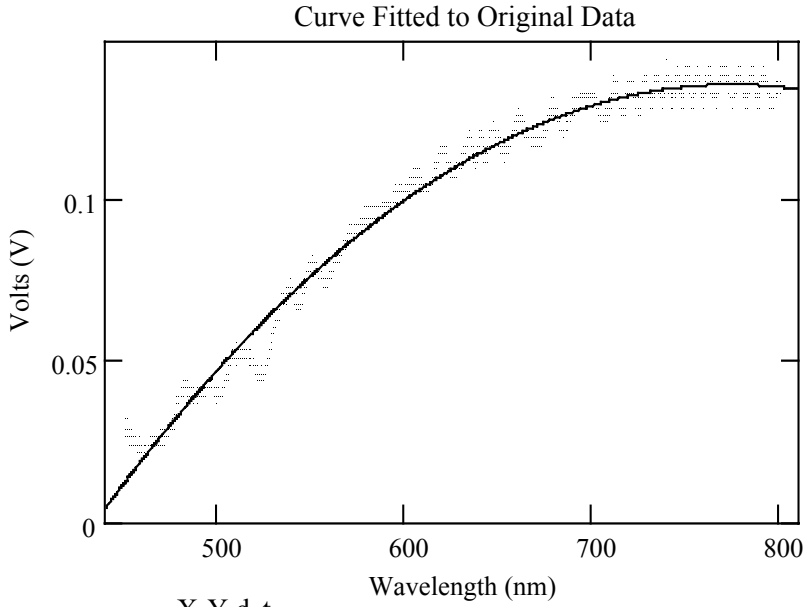

Figure 4.5: Data taken and fitted curve at 2700K with 120K resistance

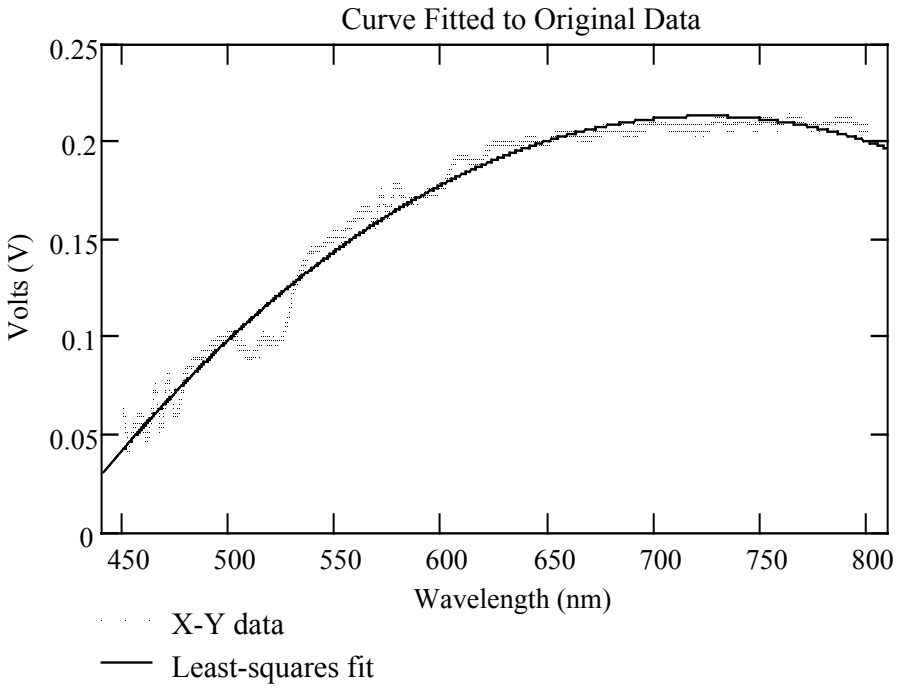

Figure 4.6: Data taken and fitted curve at 2700K with 265K resistance

Consequently, the data sets of the final method were chosen for the evaluation of the system.

All calculations and data analysis are performed with use of MathCAD program*. The figures above show original data recorded during the experiment, as well as the curve fitted to these data. The curves are fitted, after second order polynomial regression with least squares fit. This curve is used to produce Voltage versus Wavelength graphs, and in calculations. Next figures give the produced curve with output equation of polynomial regression.

* See Appendix B for an example calculation algorithm

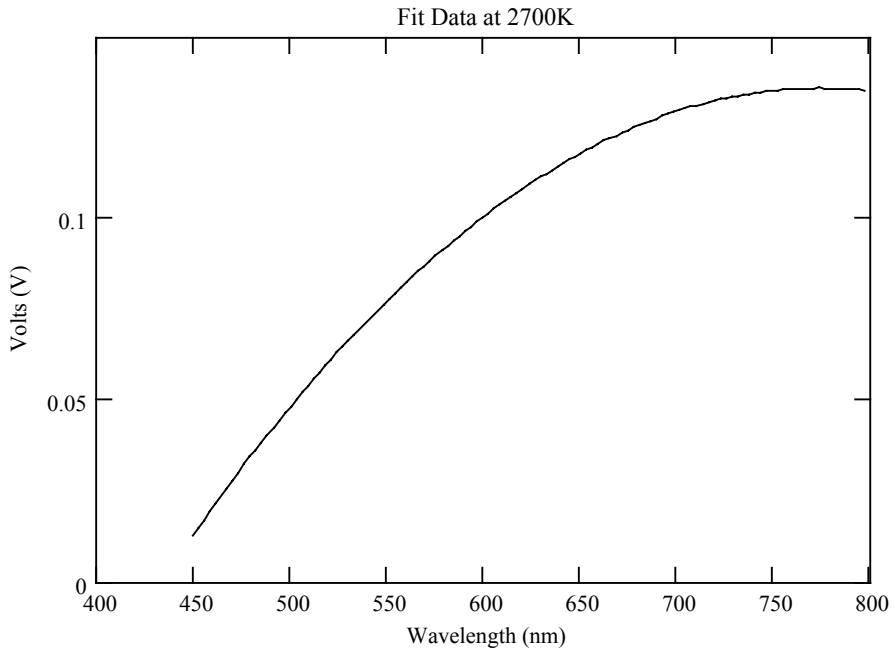

Figure 4.7: Fitted data curve reproduced versus wavelength at 2700K with 120K resistance

4.2.3 Spectral Dependence of The Absolute Photon Flux of Source

The spectral radiant exitance with respect to wavelength of a blackbody with known temperature can be found using Plancks equation

$$M_{\lambda} = \frac{3.745 \cdot 10^{8}}{\lambda^{5}} \frac{1}{e^{\frac{14388}{\lambda . T}} - 1} \qquad \text{Eq.4.1}$$

The result is in W/m^2 when wavelength is substituted in microns. Since our resolution is 3 nanometers, we have to integrate Plancks equation in 3 nm intervals from 450 nm to 800 nm for 2600K and 2700K to find the radiant exitance of a point source for certain wavelengths as in the next equation;

$$M_{\lambda} = \int_{x_i}^{x_{i+1}} \frac{3.745 \cdot 10^{8}}{\lambda^{5}} \cdot \frac{1}{e^{\frac{14388}{\lambda \cdot T}} - 1} \cdot d\lambda \qquad \text{Eq.4.2}$$

In order to evaluate the integral for changing limits, we have defined a ranged variable i and formed the limits as a series.

$$i = 0,1..117 \quad \text{and} \quad x_i = 0.44850 + \left(\frac{30.i}{10000}\right) \qquad \text{Eq.4.3}$$

The result of that evaluation is an array. All further calculations are results are also in the form of arrays. Multiplying the result of that integral, which is in the form of an array with increasing wavelength, by the area of the tungsten filament, radiant flux for certain wavelength emitted by a blackbody of same size of the tungsten filament is found (Fig.4.8.) Combining this result with emissivity ratio of tungsten with respect to a blackbody source, the radiant flux for certain wavelengths emitted by the tungsten filament is calculated. (Fig. 4.8.) Both results are illustrated below.

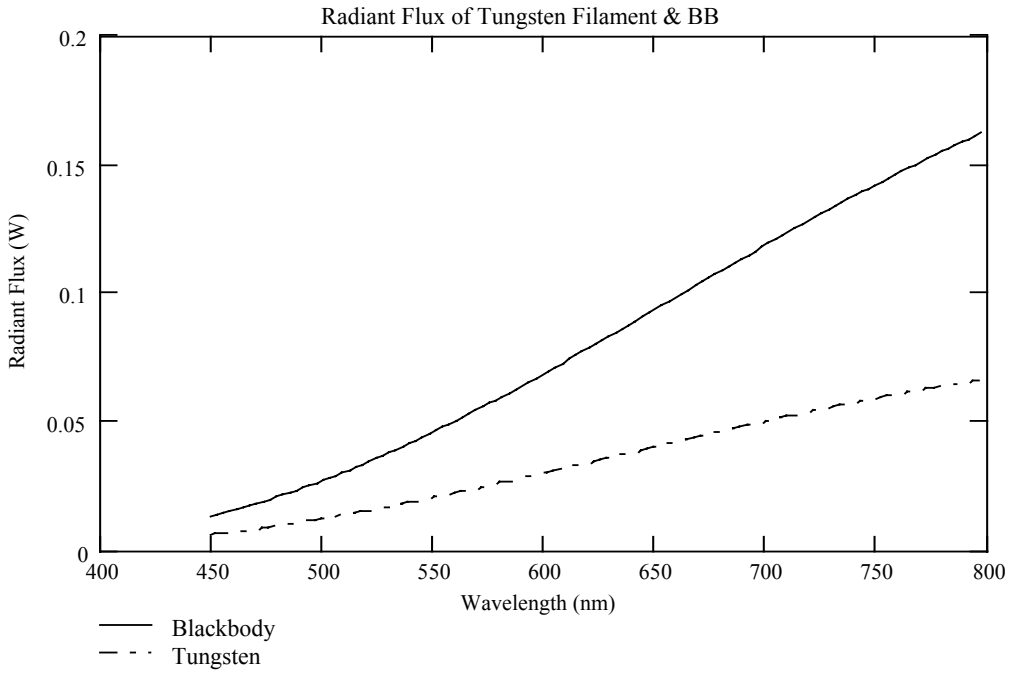

Figure 4.8: Radiant flux calculated for BB & Tungsten filament at 2600K

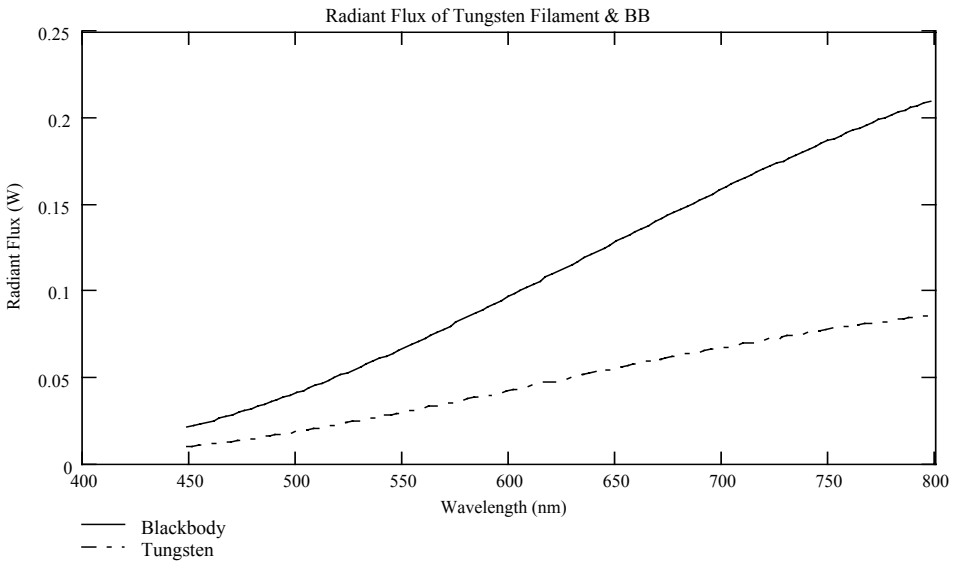

Figure 4.9: Radiant flux calculated for a BB & Tungsten filament at 2700K

The filament is approximately considered as a point source and in order to find radiant flux at the entrence slit, the percentage of slit area to that of an entire sphere with 7 cm radius is calculated and this ratio is multiplied by the previously calculated power output of tungsten filament for each wavelength, finally giving the power incident on entrence slit.

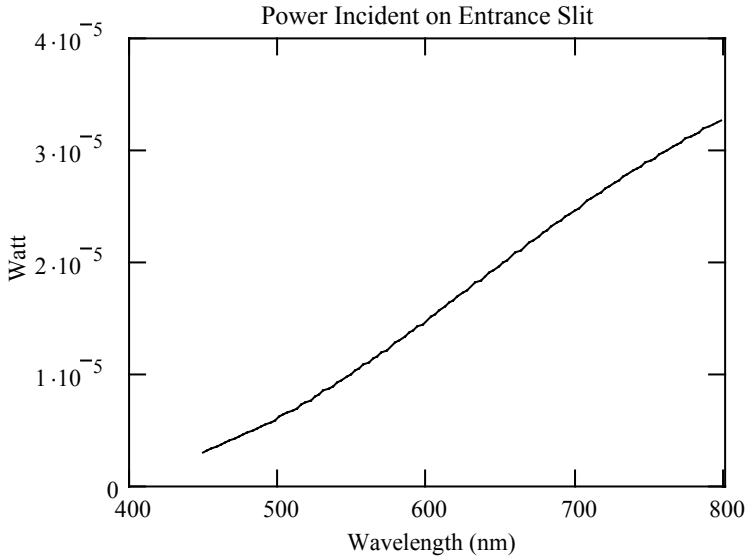

Figure 4.10: Power Incident on entrance slit at 2600K

The number of photons can then be found, just by dividing the radiant flux at the entrance slit by the energy of a single photon, again at each wavelength; which is the spectral dependence of the absolute photon flux of the calibrated lamp.

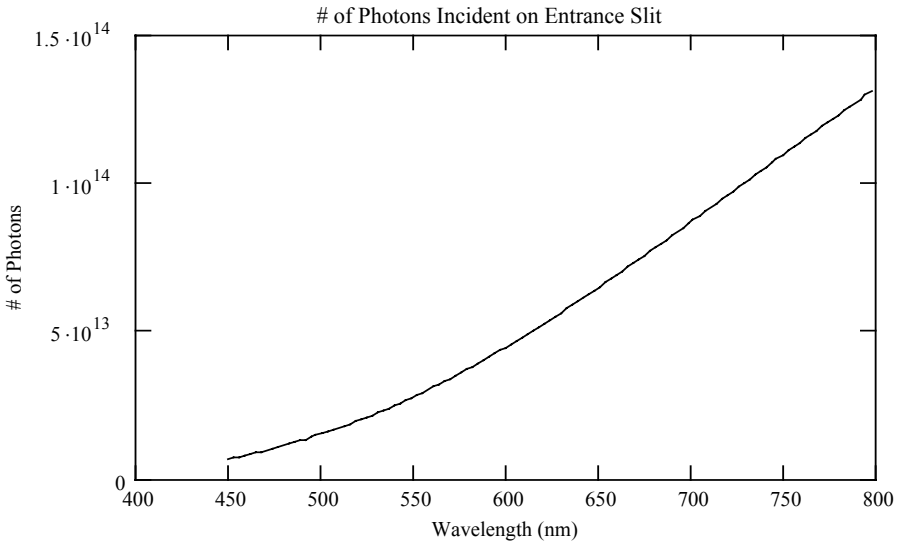

Figure 4.11: Number of photons incident on entrance slit at 2600K

4.2.4 Calibration of Diode by Comparison to The Photon Flux of The Calibrated Lamp

Photosensitivity is the ratio of radiant energy expressed in watts incident on the device, to the output photocurrent expressed in amperes. Quantum efficiency is the photocurrent divided by the number of photons incident on the device. Considering our setup, since a sensitive current measuring instrument is unavailable, the measured quantity is voltage, thus we have to replace Volts with Amperes. Dividing voltage by the power and number of photons at the entrance slit with respect to wavelength result in photosensitivity and quantum efficiency of system respectively.

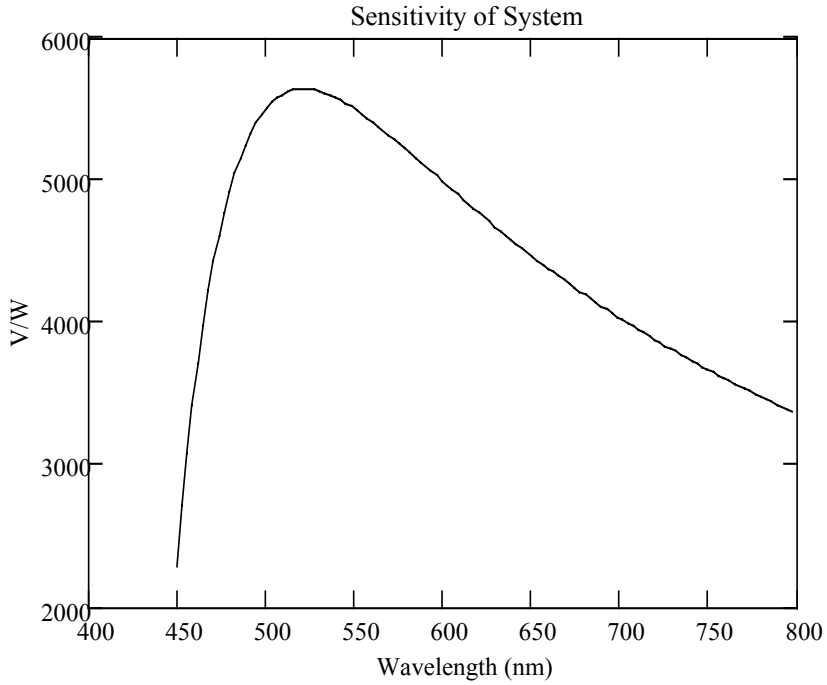

Figure 4.12: Sensitivity of sytem at 2600K

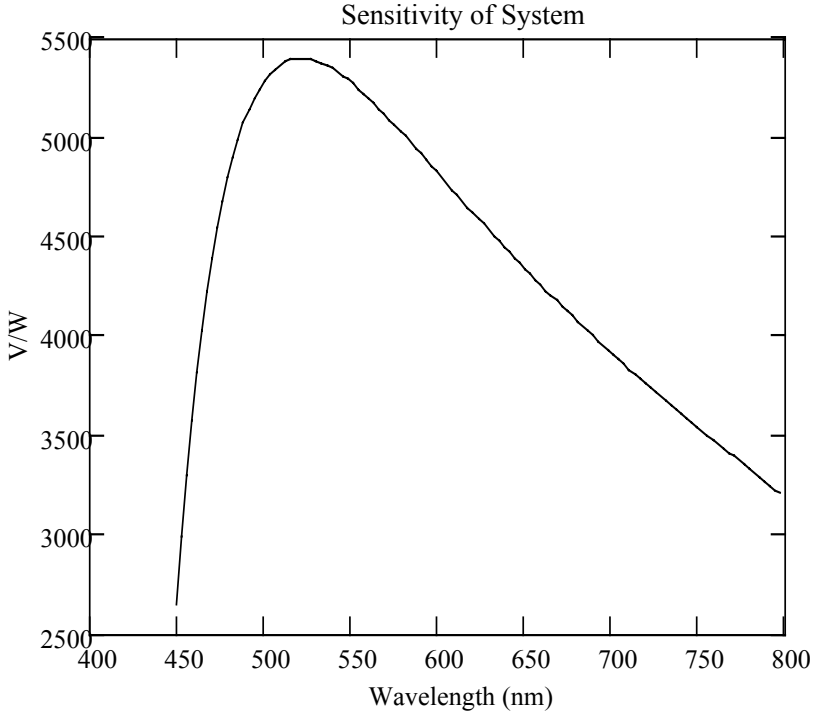

Figure 4.13: Sensitivity of sytem at 2700K

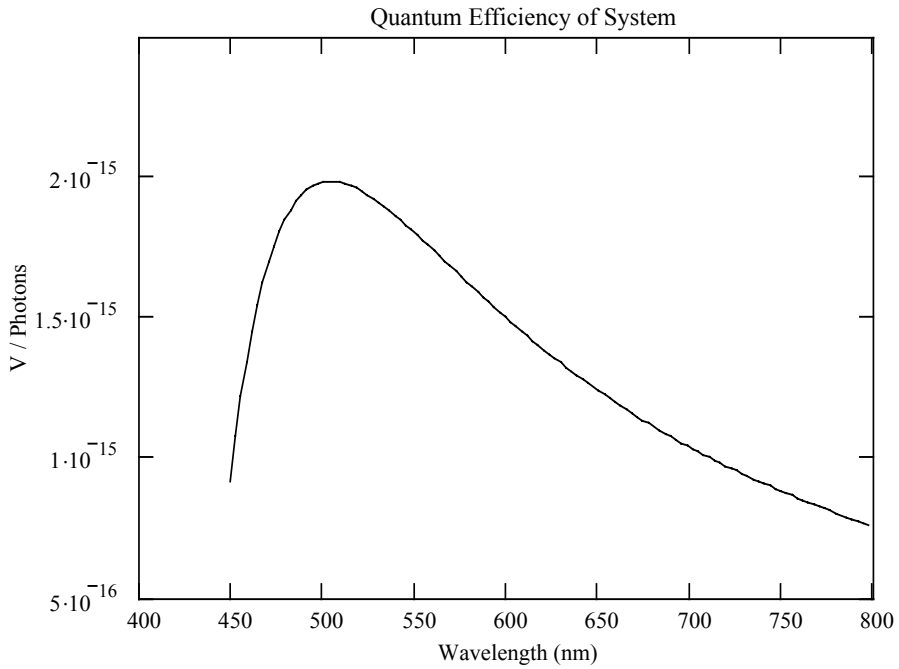

Figure 4.14: Quantum efficiency of system at 2600K

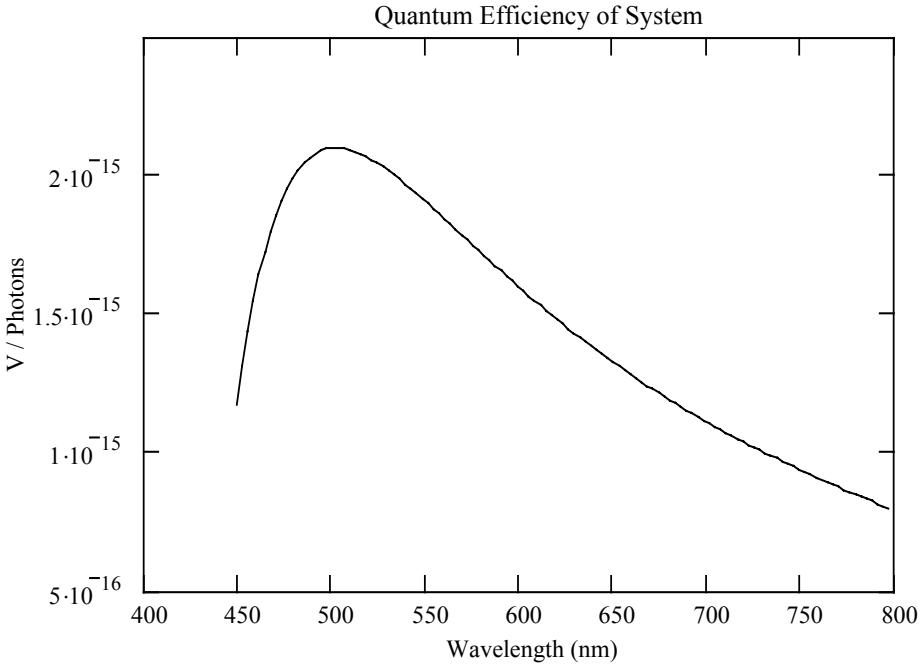

Figure 4.15: Quantum efficiency of system at 2700K

What is expected is that for different ribbon temperatures, the sensitivity and quantum efficiency of system should be the same. Because, calculated radiant energy and photon flux incident on the diode are absolute values. Division of spectral sensitivity and the quantum efficiency for different ribbon temperatures should equal unity.

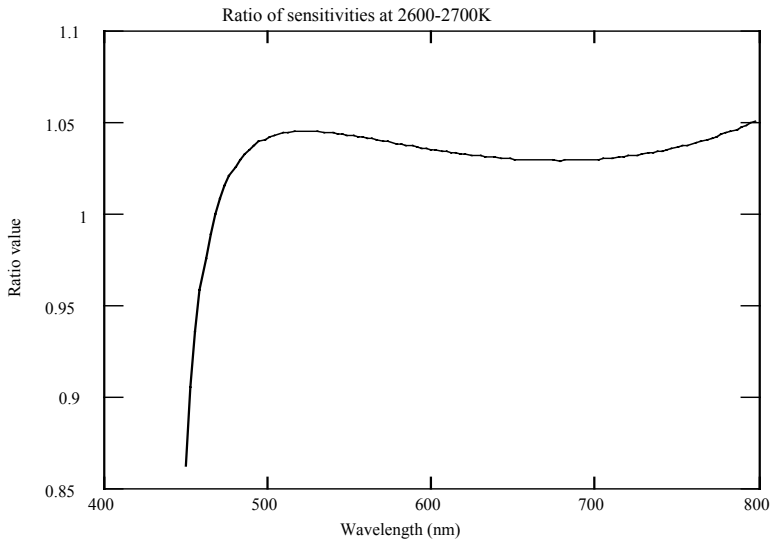

Figure 4.16: Ratio of sensitivity at 2600K to that of at 2700K

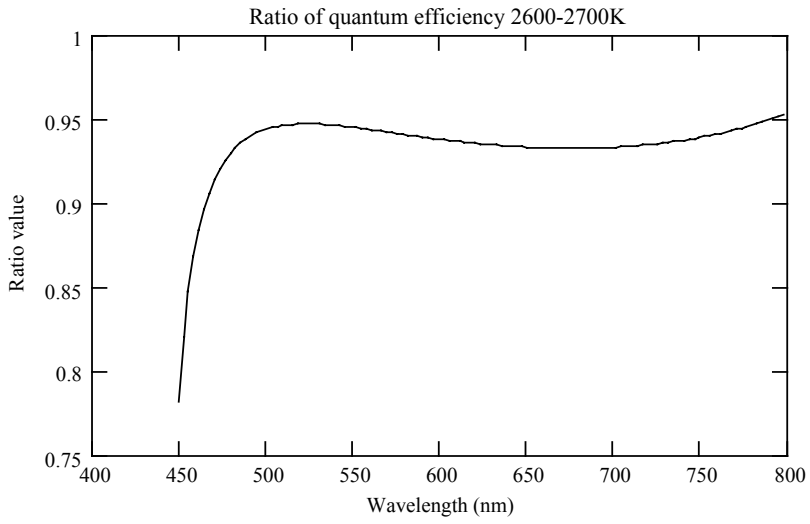

Figure 4.17: Ratio of quantum efficiency at 2600K to that of at 2700K

4.2.5 Determination of Transmission and Reflection Coefficients

The optical component of which the transmission coefficient is to be determined is a piece of glass. The transmission coefficient can be found simply by comparing data measured with and without the component in front of the entrence slit. In other words, the ratio of measured data curves with and without the glass in front of the entrence slit gives the transmission coefficient of the component with respect to the wavelength.

$$R_{T2600\_T2700\_120} := \overrightarrow{\left(\frac{T_{fit\_2600\_120}}{T_{fit\_2700\_120}}\right)} \qquad \text{Eq.4.4}$$

Again, using above array calculation in MathCAD, recorded voltage values for two different cases, with and without the piece of glass in front of entrance slit, at each wavelength are divided one by one at both 2600K and 2700K. Then ratio of two transmission arrays is taken.

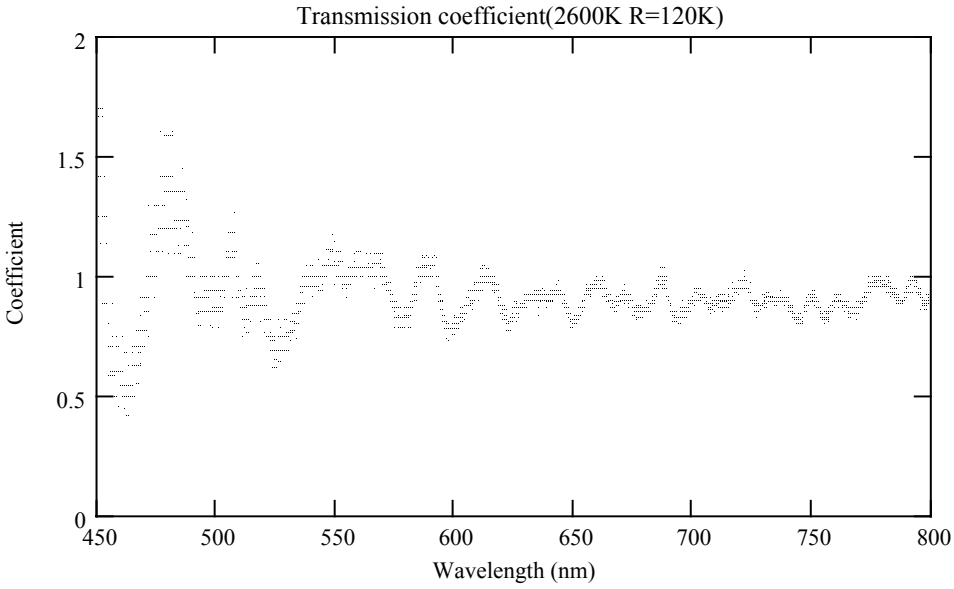

Figure 4.18:Transmission coefficient data (2600K, R=120K)

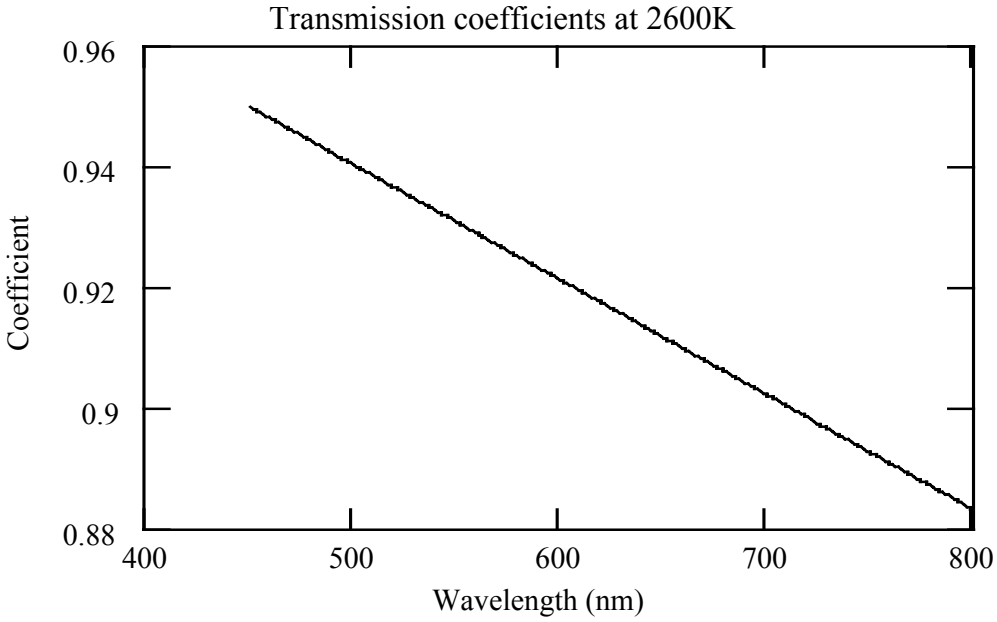

Figure 4.19: Fitted Transmission coefficient vs wavelength at 2600K

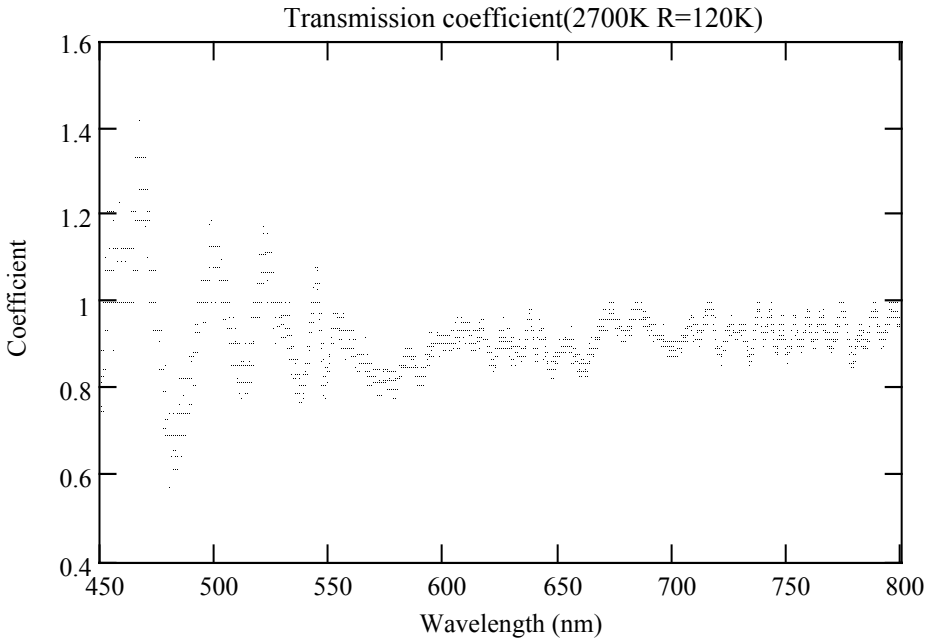

Figure 4.20: Transmission coefficient data (2700K, R=120K)

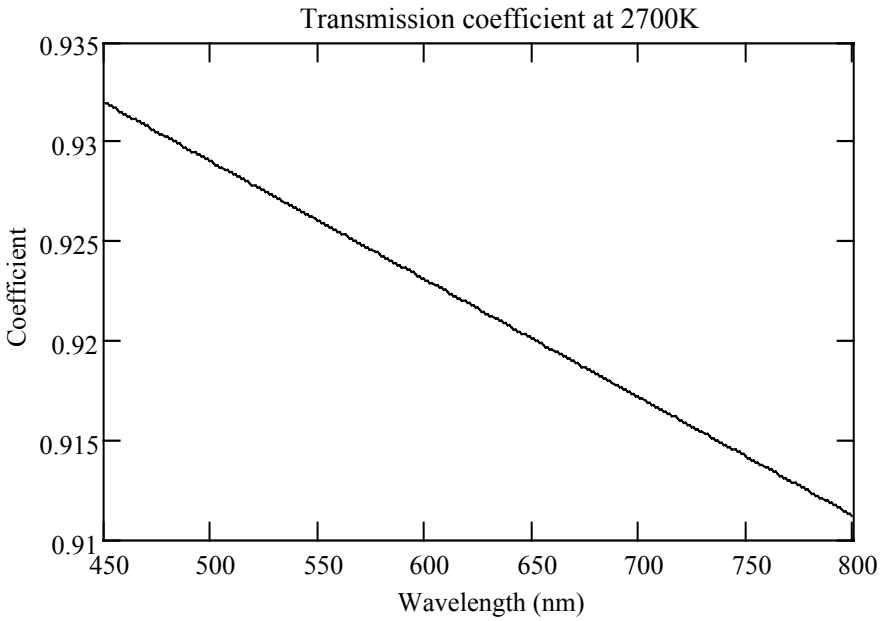

Figure 4.21: Fitted Transmission coefficient vs wavelength at 2700K

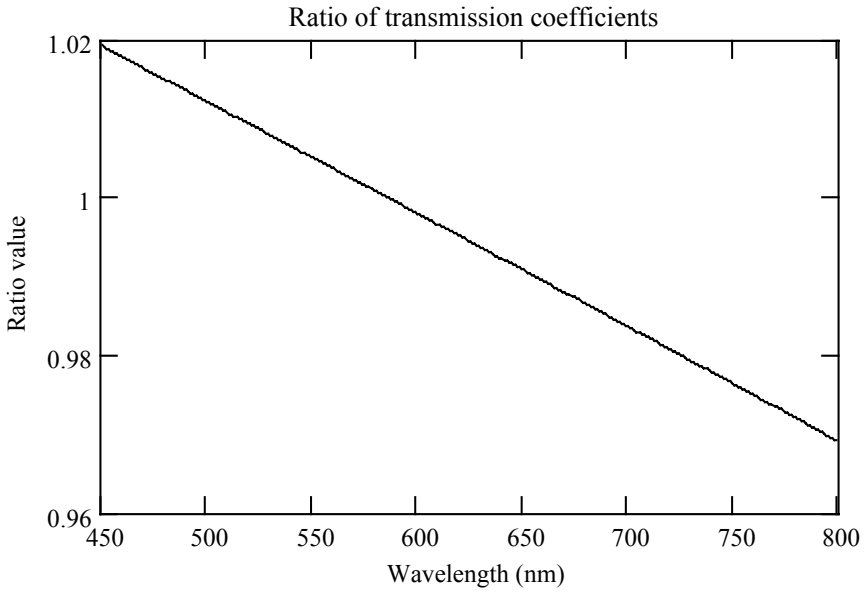

Figure 4.22: Ratio of transmission coefficients at 2600K and 2700K

For above introduced three parameters, sensitivity, quantum efficiency and transmission coefficient are all expected to remain constant when ribbon temperature is changed. Taking the ratio of sensitivity and quantum efficiency of system and transmission coefficients of glass at 2600K to those at 2700K, all three ratios have to give unity. In our results, this is not the case. We have a deviation from the expected. Especially between 450 to 500 nanometers, amount of deviation is much higher. Neglecting that region deviations are approximately 5 percent and acceptable. For example, the ratio of coefficients is found to vary between 1.02 and 0.96. We have unity at around 580 nanometers.

CHAPTER 5

CONCLUSION

The aim was to pick best choice among several light sources and to install a data logger for the optical experimental setup to be constructed. The setup should be used to investigate plasma parameters or optical properties of components such as lenses and windows of other experimental arrangements used in plasma investigations. As a whole, objectives are achieved. The light source for different applications is determined and reported. Data acquisition system is installed and working with performance. The setup is constructed and, although there is a lower limit for the voltage approximately at 5 mV, is ready for further experiments.

The light source options are analyzed and it is decided that Tungsten Strip Lamp is the best choice for our purpose in that absolute photon flux can be calculated. Considering results of primary inspections, range of data acquisition system was adjusted. Use of signal conditioning circuits was discussed. Since the output of photodiode is low, a circuit is constructed, however the noise level of data is increased. A simpler but more effective method is used. A high resistance is connected across the legs of photodiode and voltage across it is measured. Also, an algorithm of data analysis is prepared and a PC based data acquisition system that can be implemented to other setups is installed.

The results of the experiment are not satisfactory between 450 to 500 nm where the system turn out to be inefficient. The significant variation of data in this range makes it impossible to calculate any value. The inconsistency in this range is disregarded. In addition to these, although only dynamic part of system, the grating, fits our range of interest, since the efficiency of gratings used in the monochromators could not be obtained from the manufacturer, we have very little knowledge about the errors due to this factor. Inspecting a very similar grating of which the properties are known but not available in the labaratory, we realized that efficiency of grating decreases rapidly with increasing wavelength. This may be the reason for inconsistency in our data.

We expect to obtain same sensitivity and quantum efficiency curves for different temperature values of the tungsten filament. The ratio of these is not exactly the same for our setup, however, the sensitivity curve deviate from 1 up to 1.05 between 500 to 800 nm. This is due to many effects, which contribute to the system as an error source. The deviation is a little less than 5 percent, which can be considered in the limits. The error in calculations, experimental instruments are considered as a whole, and they add up in total to a reasonable fraction of data recorded.

The work happened to be an elementary study of optical experimental systems. It actually has been a good preparation period for future experiments covering plasma investigations. We earned familiarity to equipment, software and to conduction of experiments starting from the very beginning stages. All problems we encountered increased our level of experience.

At the end, the optical setup we intended to construct is ready to use for further experiments with a small deficiency.

REFERENCES

1. Levi, Leo, Applied Optics: A guide to Optical System Design, John Wiley and Sons. 1968,
2. Philips Lighting Catalog 2003
3. Diefenderfer, A.James, Principles of Electronic Instrumentation, W.B.Saunders Comp,
4. De Vos, A New Determination of Emissivity of Tungsten Ribbon, Physica XX, 1954 pp 690-714
5. Dolan, Thomas James, Fusion Research: Principles, Experiment ant Technology, Pergamon Press, c1982
6. Jerry Workman Junior, Art W. Springsteen, Applied Spectroscopy , Academic Press, c1998
7. 1979Hamamatsu Optical Instruments Catalog, 2001
8. Austerlitz, Howard, Data Acquisition Techniques Using Personal Computers, Academic Press, 1991
9. Buchanan, William, Applied PC Interfacing, Graphics and Interrupt, Addison Wesley Longman, 1986
10. Borland International, Borland Pascal With Objects, 1992
11. Brown, Steven D., Computer Assisted Analytical Spectroscopy, Chichester ; New York : Wiley, c1996
12. Allan Billings, Optics, Optoelectronics and Photonics, Prentice Hall,1983
13. Hetch, Eugene, Optics, Addison-Wesley Pub. Co. 1974
14. Optical Society of America, Handbook of Optics, McGraw-Hill, 2001

15. Improvement to monochromator spectral calibration using a tungsten strip lamp, Hannspeter Winter and E.W.P. Bloemen, J.Phys. E: Sci. Instrum Vol.15,1982
16.Simple designes to measure efficiency of different type of monochromators, O.Prakash, R.S. Ram, J.Optics (Paris), Vol.27. 1996, pp 241-245
17. Effect of the geometrical parameters on an absolute calibration, J.P.Lanquart, J.Phys D: Appl. Phys 19 (1986),pp 2043-2049
18. Simple method of spectrometer-detector sensitivity calibrations in the 210-1150nm range, A.A. Fataev, E.H.Fint, A.M. Pravilov, Meas. Sci. Technology, 10 (1999), pp 182-185

APPENDIX A

RESULTS OF DATA TAKEN WITH OTHER INSTRUMENTS

In the setup Hamamatsu S2506-02 Si PIN photodiode was introduced as the detector. In addition, two more type of diode were available, namely Hamamatsu S1133-14 and S1227-33BQ Si photodiodes. The experimental procedure was repeated several more times with diode S2506-02 subtituted by other two one by one. Also, one more monochromator was available: Jarrell Ash Monospec50. More data was recorded combining all diodes and Monospec50. Next figures belong to results of some of these data.

A.I. Diode Substitution

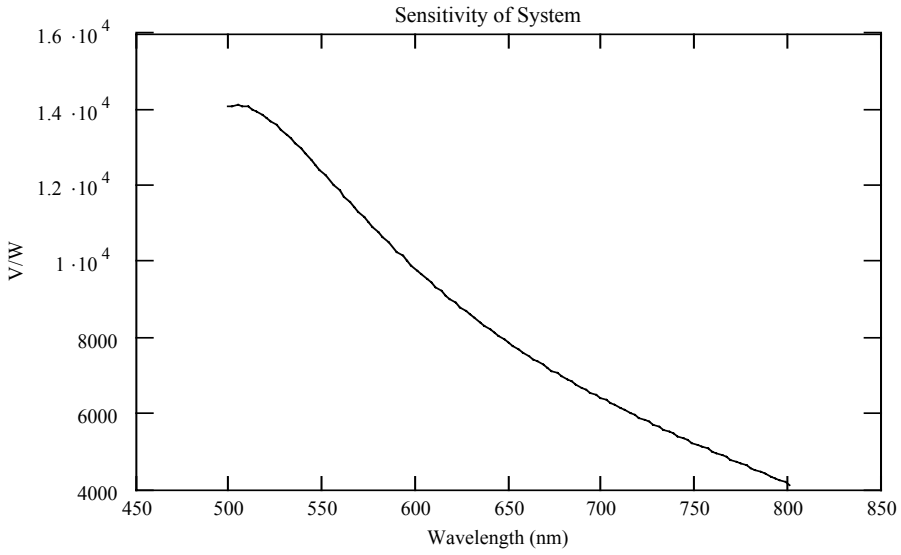

Figure A.1: Sensitivity with S1133-14 Diode at 2700K with R=265K

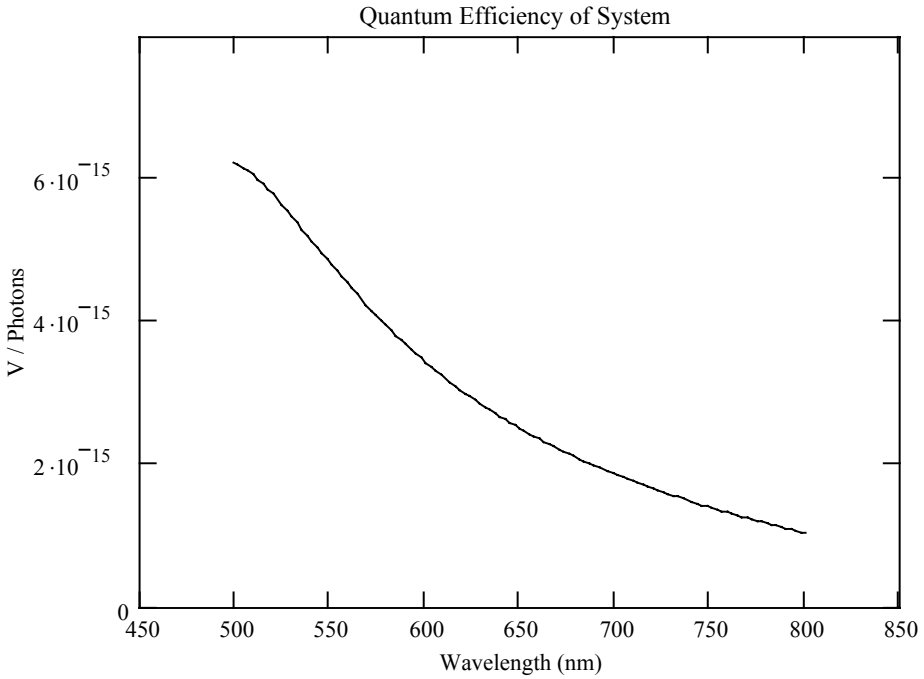

Figure A.2: Quantum efficiency with S1133-14 Diode at 2700K with R=265K

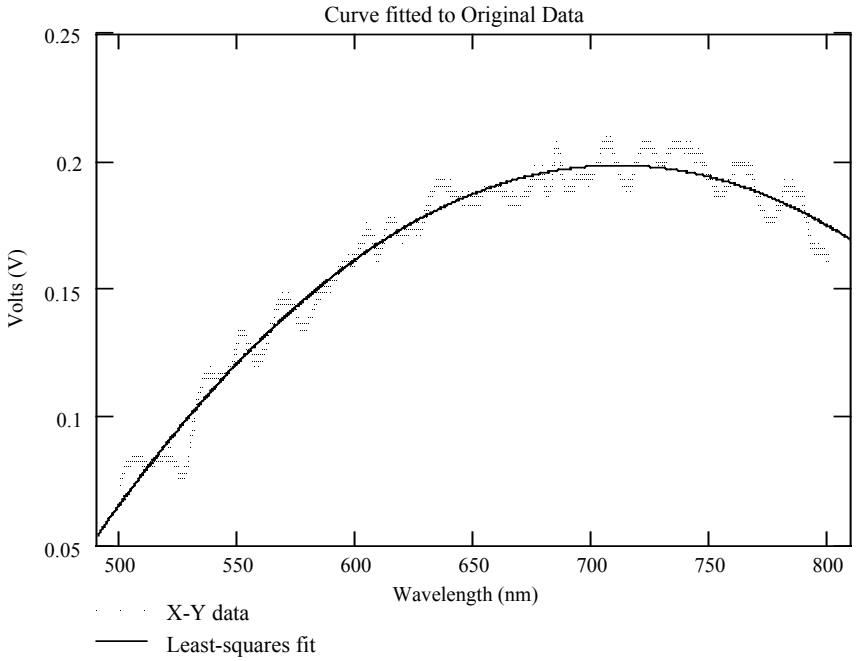

Figure A.3: Data and curve fitted with S1133-14 Diode at 2700K with R=265K

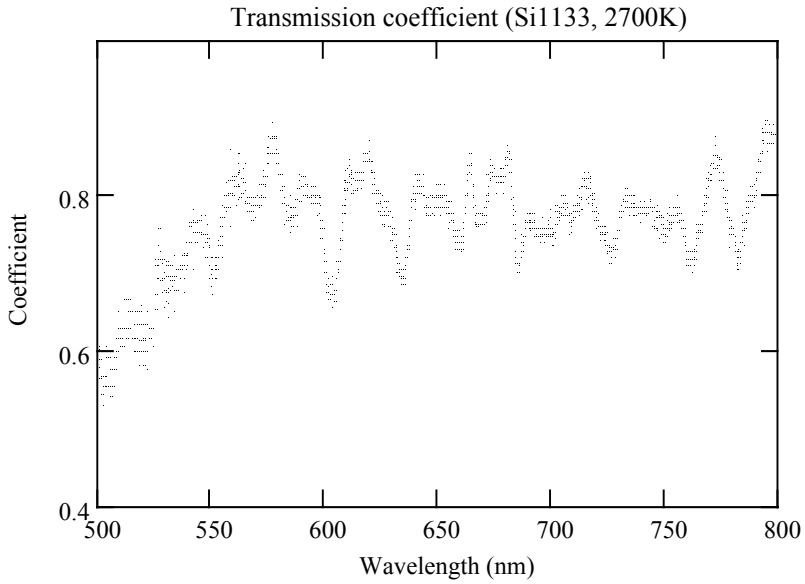

Figure A.4: Transmission coefficient with S1133-14 Diode at 2700K (R=265K)

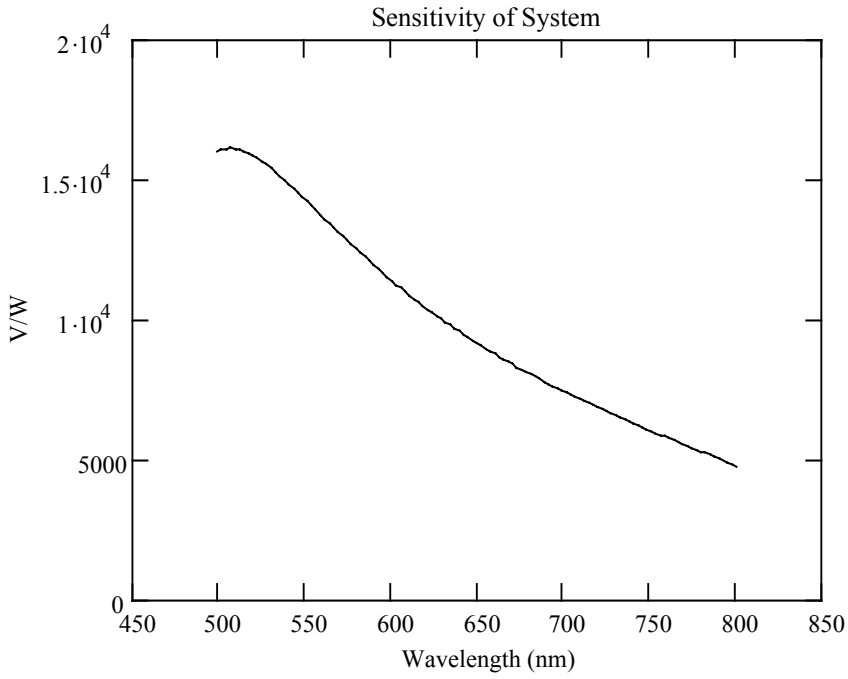

Figure A.5: Sensitivity with S1227-33BQ Diode at 2700K with R=265K

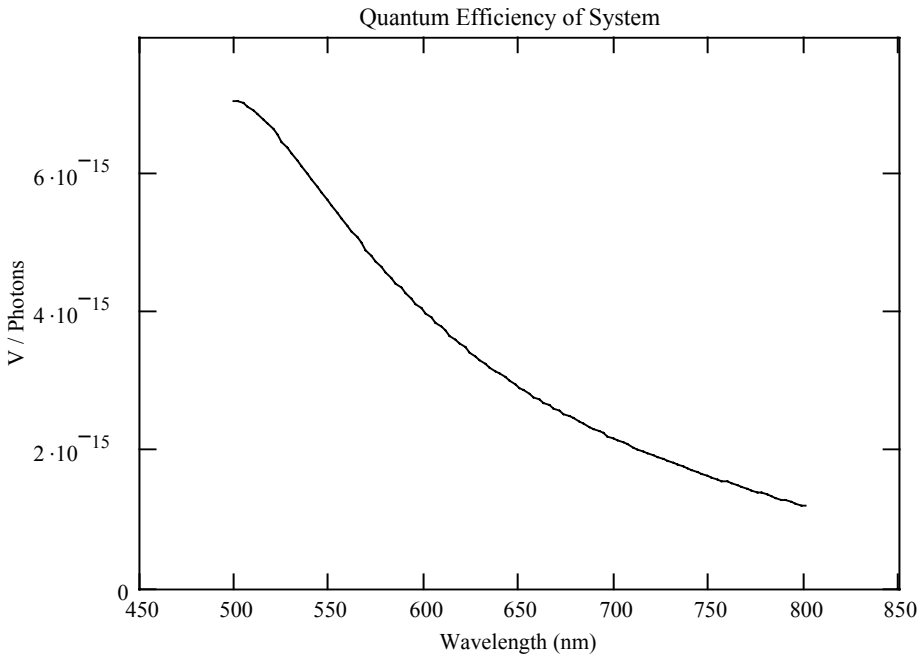

Figure A.6: Quantum efficiency with S1227-33BQ Diode at 2700K (R=265K)

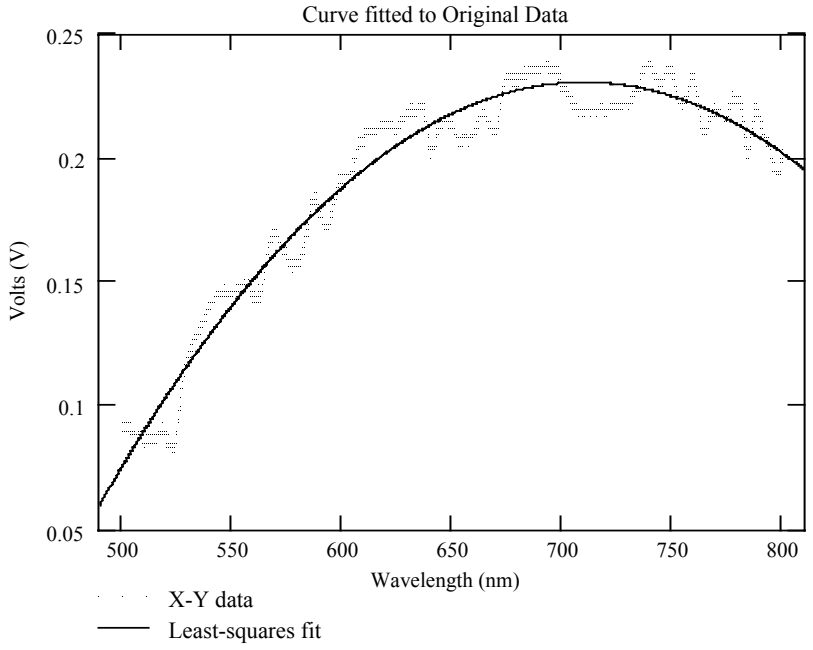

Figure A.7: Data and fitted curve with S1227-33BQ Diode at 2700K (R=265K)

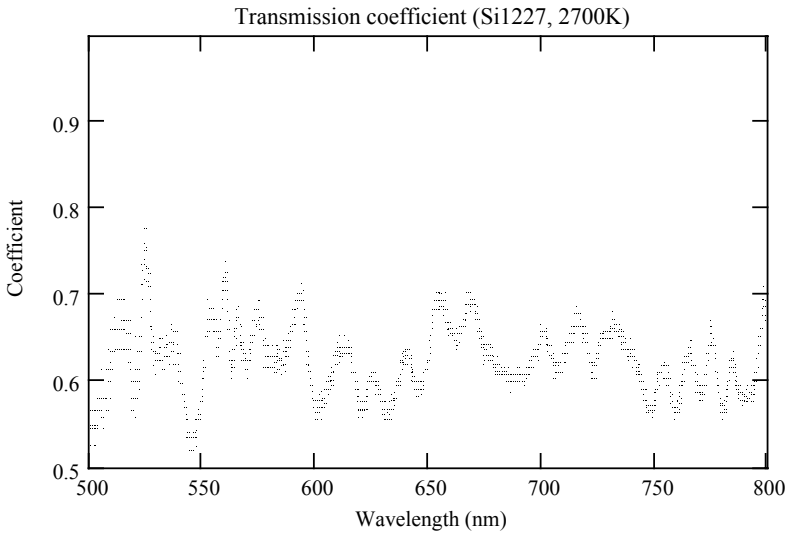

Figure A.8: Transmission coefficient with S1227-33BQ Diode at 2700K (R=265K)

A.II. Setup Including Monospec50

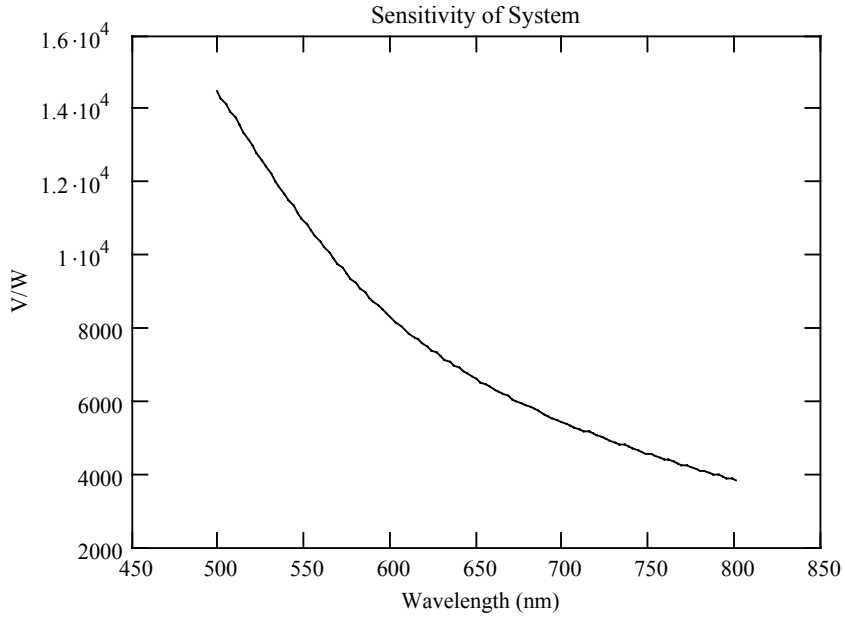

Figure A.9: Sensitivity with Monospec50 and S1133-14 Diode at 2700K

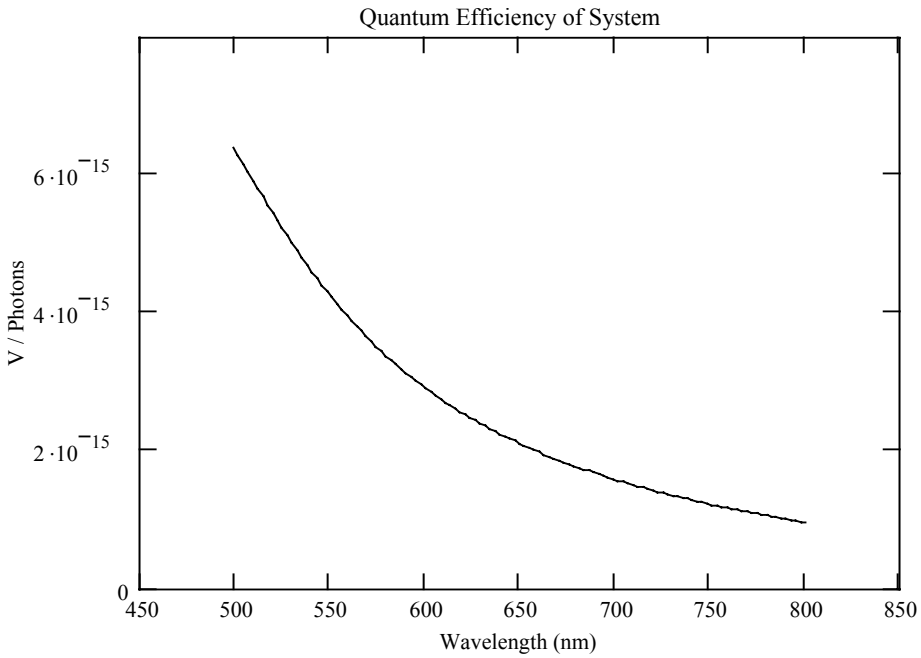

Figure A.10: Quantum efficiency with Monospec50 and S1133-14 Diode at 2700K

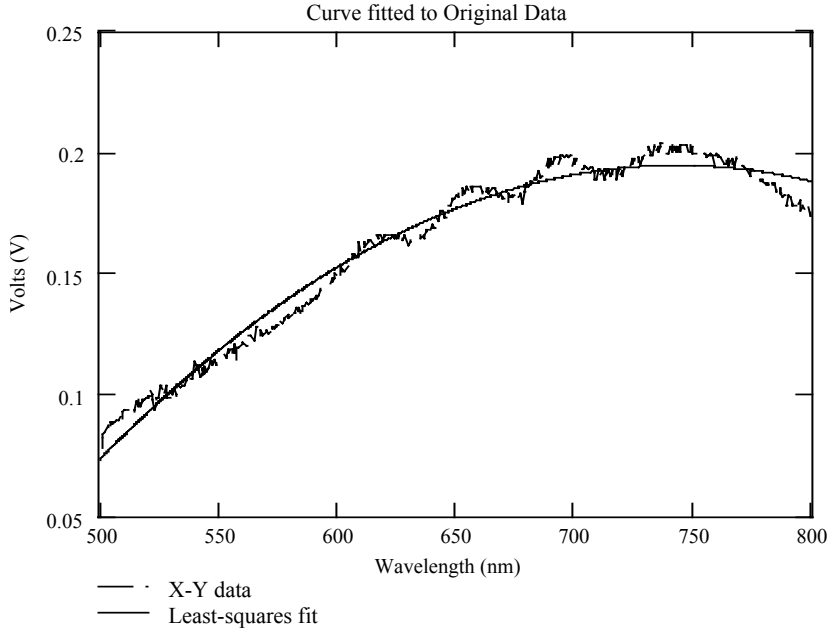

Figure A.11: Data and curve fitted with Monospec50 and S1133-14 Diode at 2700K

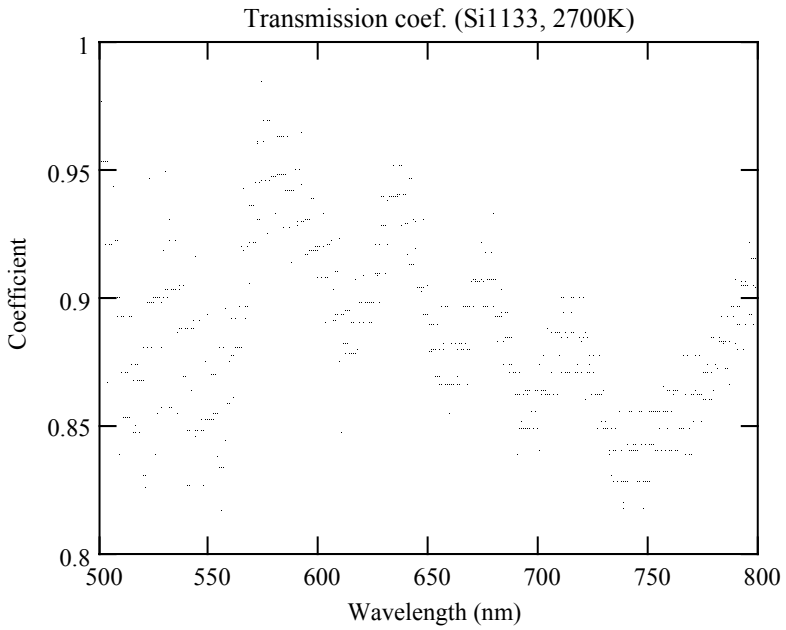

Figure A.12: Transmission coefficient with Monospec50 and S1133-14 Diode at 2700K

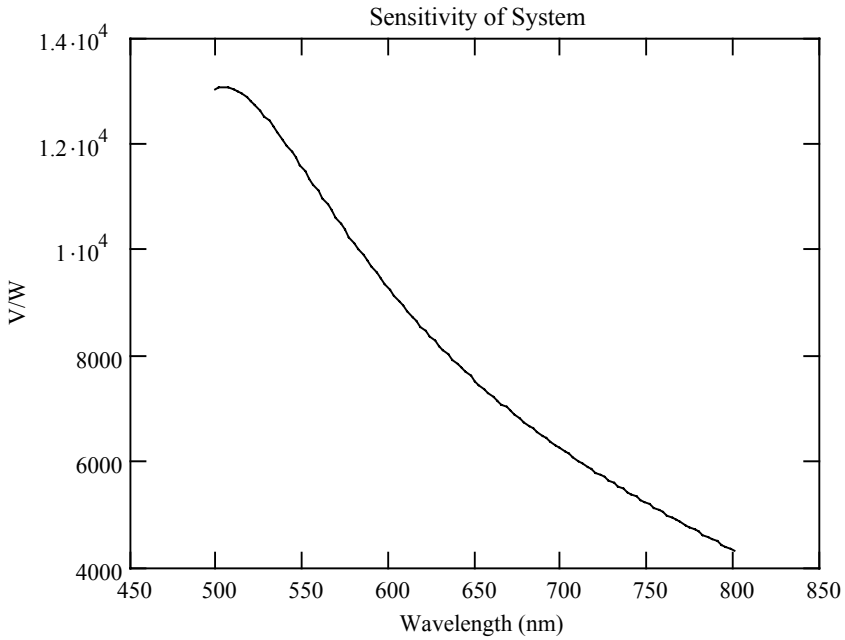

Figure A.13: Sensitivity with Monospec50 and S1227-33BQ Diode at 2700K

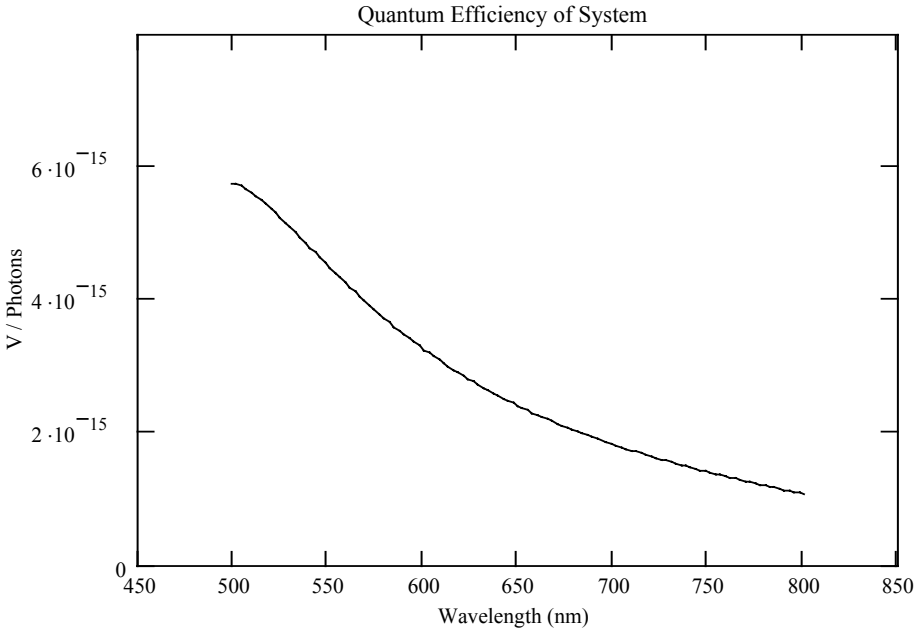

Figure A.14: Quantum efficiency with Monospec50 and S1227-33BQ Diode at 2700K

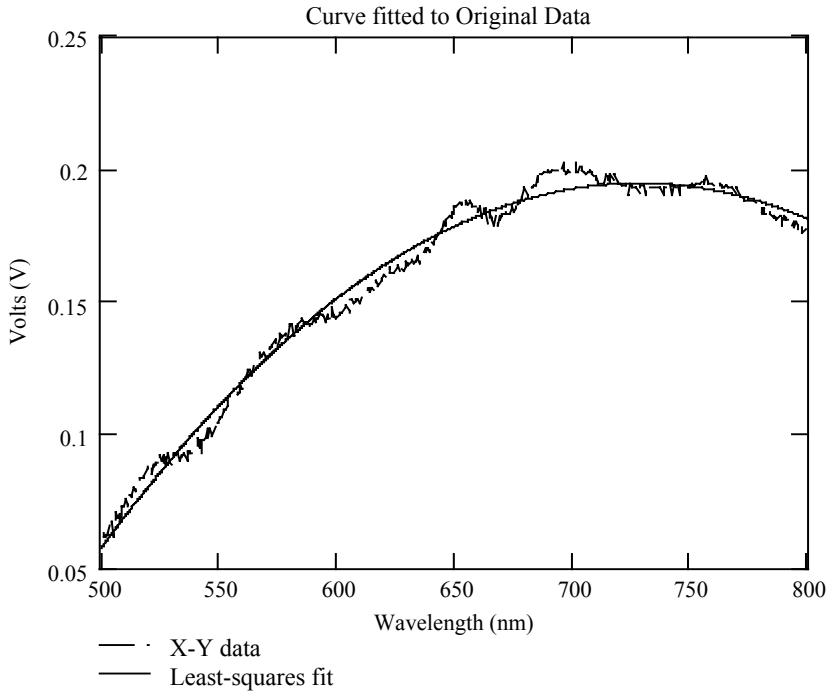

Figure A.15: Data and curve fitted with Monospec50 and S1227-33BQ Diode at 2700K

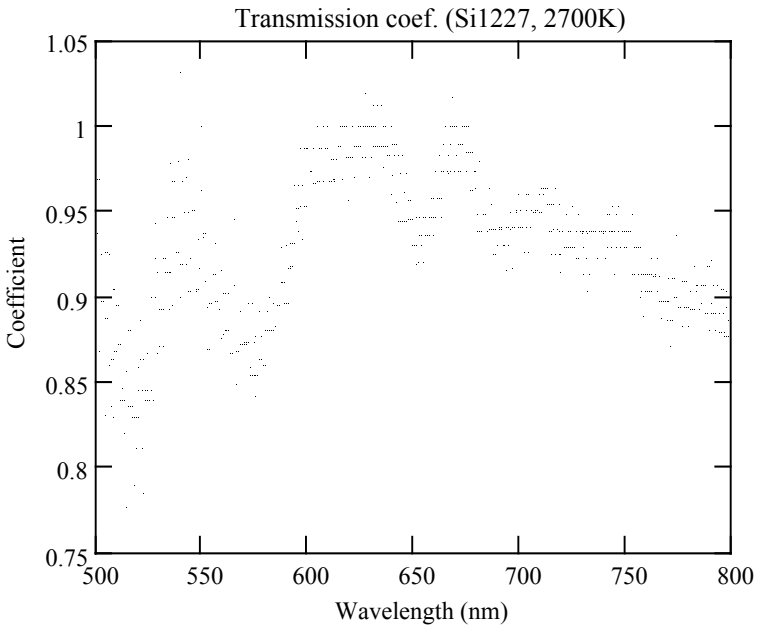

Figure A.16: Transmission coefficient with Monospec50 and S1227-33BQ Diode at 2700K

APPENDIX B

DATA ANALYSIS ALGORITHM

Radiant flux calculation from Planck Equation.

$i := 0, 1 .. 117$

$$x_i := 0.44850 + \left(\frac{30 \cdot i}{10000}\right)$$

$$W2700_i := \left\| A \leftarrow \int_{x_i}^{x_{i+1}} \left[\frac{3.745 \cdot 10^8}{(z)^5}\right] \cdot \left(\frac{1}{e^{\frac{14388}{z \cdot 2700}} - 1}\right) dz \quad \text{if } i < 117 \right\| A$$

Resulting arrays for Power (W_{2700}) of BB at 2700K and x values (wavelength).

$W_{2700} =$

	0
0	438.159
1	458.418
2	479.224
3	500.576
4	522.473
5	544.912
6	567.891
7	591.408

$x =$

	0
0	0.4485
1	0.4515
2	0.4545
3	0.4575
4	0.4605
5	0.4635
6	0.4665
7	0.4695

W_{2700} is in W/m^2 and x is in microns.

Multiplying power with area of filament gives radiant flux of a BB with same area of Tungsten ribbon: ($S_{filament\_area\_2700K}$)

$$S_{filament\_area\_2700K} := 48 \cdot 10^{-6} \cdot Y$$

$S_{filament\_area\_2700K} =$

	0
0	0.021
1	0.022
2	0.023
3	0.024
4	0.025
5	0.026
6	0.027
7	0.028

Knowing the emissivity of tungsten with respect to a BB from DeVos graph, we can calculate radiant flux of tungsten filament. First we digitized emissivity curves and obtained a wavelength depended equation from these digitized data.

E :=

	0	1
0	0.402	0.466
1	0.405	0.465
2	0.408	0.464
3	0.411	0.464
4	0.413	0.464
5	0.416	0.463

Digitized data
coloumn 0: wavelength in microns
coloumn 1: emissivity ratio

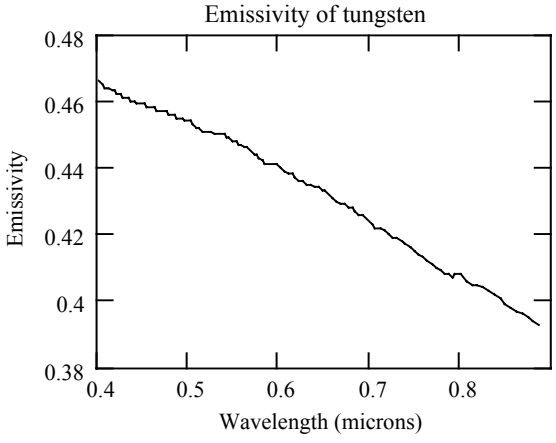

Figure B.1: Emissivity of tungsten. Digitized and reproduced from DeVos' graph

Then an equation of first order polynomial that fits this curve was obtained using polynomial regression with least square fit method, already present in MathCAD software. Equation of fitting line and resulting array are;

$T_{fitted\_emsvty} := -0.15 \cdot x + 0.528$

$T_{fitted\_emsvty} =$

	0
0	0.460725
1	0.460275
2	0.459825
3	0.459375
4	0.458925
5	0.458475

Previously calculated BB radiant flux multiplied by emissivity ratio is the flux from tungsten fialment.

$F_{tun\_fil\_output\_2700K} := \overrightarrow{\left(T_{fitted\_emsvty} \cdot S_{filament\_area\_2700K}\right)}$

$F_{tun\_fil\_output\_2700K} =$

	0
0	$9.69 \cdot 10^{-3}$
1	0.01
2	0.011
3	0.011
4	0.012
5	0.012

Radiant flux of filament

Having the ratio of slit area to complete sphere surface of radius 7 cm, radiant flux at the slit is obtained.

$S_{slit\_2700K} := \left(F_{tun\_fil\_output\_2700K} \cdot 30 \cdot 10^{-6}\right) \div (0.061)$

$S_{slit\_2700K} =$

	0
0	$4.765 \cdot 10^{-6}$
1	$4.981 \cdot 10^{-6}$
2	$5.202 \cdot 10^{-6}$
3	$5.428 \cdot 10^{-6}$
4	$5.66 \cdot 10^{-6}$
5	$5.898 \cdot 10^{-6}$

Radiant flux incident on entrence slit

Dividing this flux by energy of a single photon at each wavelength, number of photon incident on entrence slit is found.

$$N_{ph\_slit\_2700K} := \frac{\overrightarrow{\left(\lambda \cdot S_{slit\_2700K}\right)}}{\left(6.62 \cdot 10^{-34} \cdot 3 \cdot 10^{8}\right)}$$

$N_{ph\_slit\_2700K} =$

	0
0	$1.077 \cdot 10^{13}$
1	$1.134 \cdot 10^{13}$
2	$1.192 \cdot 10^{13}$
3	$1.252 \cdot 10^{13}$
4	$1.314 \cdot 10^{13}$
5	$1.378 \cdot 10^{13}$

At 2700K we know power incident on entrence slit. Now, we introduce data.

H :=

	0	1
0	0	0.029
1	0	0.027
2	0	0.029
3	0	0.029
4	0	0.032

Data table

Coloumn 0: Time (s)

Coloumn 1: Voltage (V)

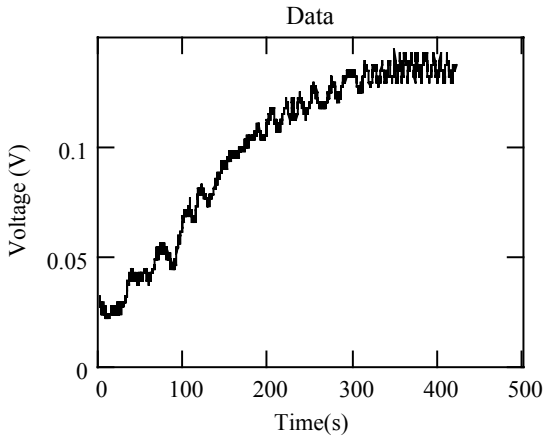

Graph of data as recorded

Figure B.2: Plot of raw data submitted into table

We use second order polynomial regression with least square fit to produce an equation to be used in further calculations.

$$V_{voltage\_fit} := -8.177\times 10^{-7}\cdot t^2 + 6.367\times 10^{-4}\cdot t + 0.012$$

$V_{voltage\_fit} =$

	0
0	0.013
1	0.015
2	0.017
3	0.019
4	0.022
5	0.024

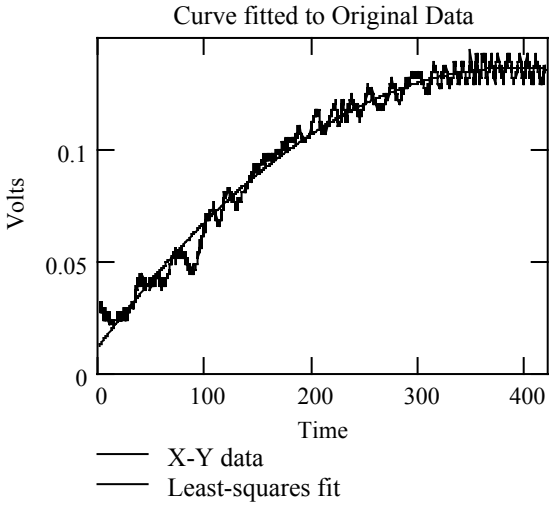

Figure B.3: Data points and curve fitted

$$S_{sensitivity\_2700K\_R1} := \overrightarrow{\left(\frac{V_{voltage\_f}}{P_{slit\_power}}\right)}$$

Equation for sensitivity of system

Fitted voltage per power

$$QE := \overrightarrow{\left(\frac{V_{voltage\_f}}{N_{photon}}\right)}$$

Quantum efficiency of system

Fitted voltage per photon

Then graphs are automatically plotted.

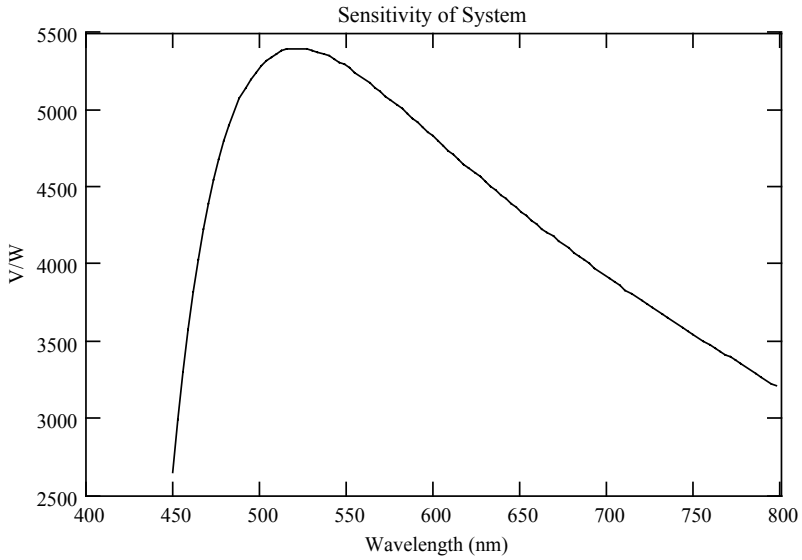

Figure B.4: Plot of sensitivity of system

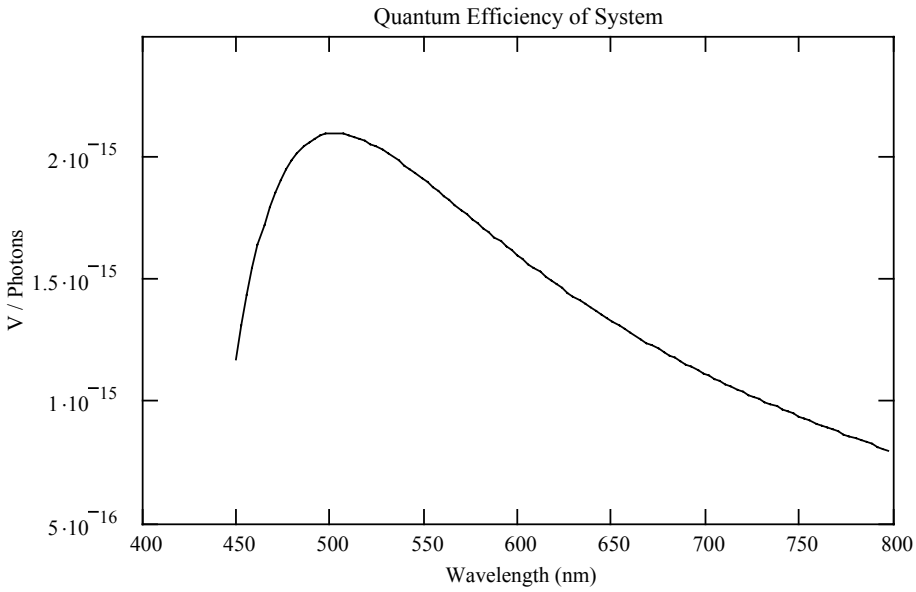

Figure B.5: Plot of quantum efficiency of system

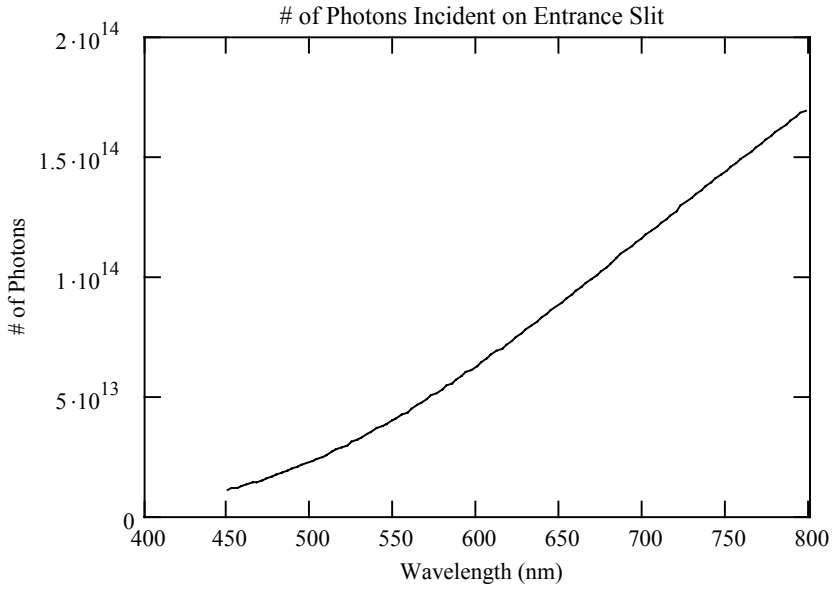

Figure B.6: Plot of number of photons incident on entrence slit

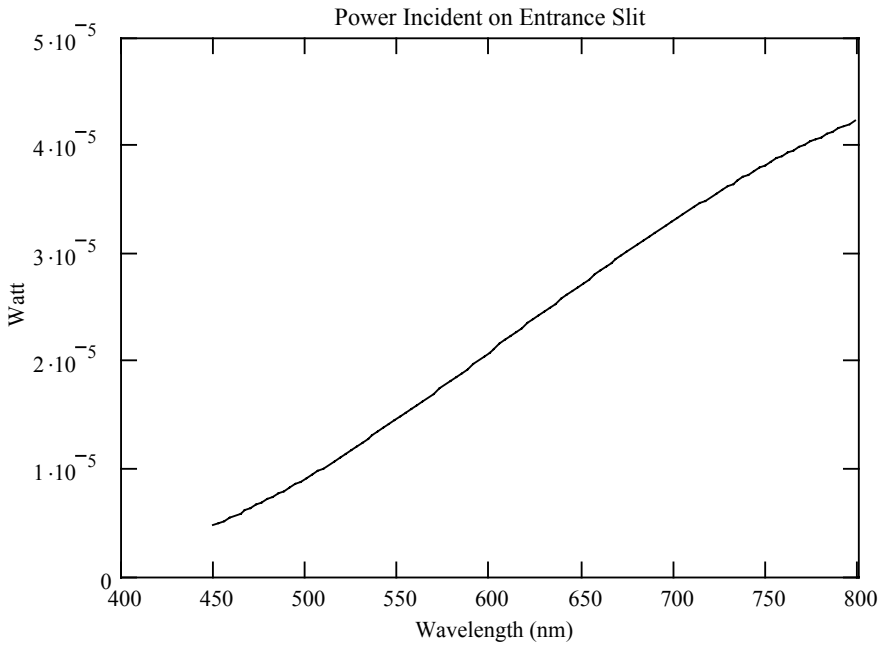

Figure B.7: Plot of power incident on entrence slit

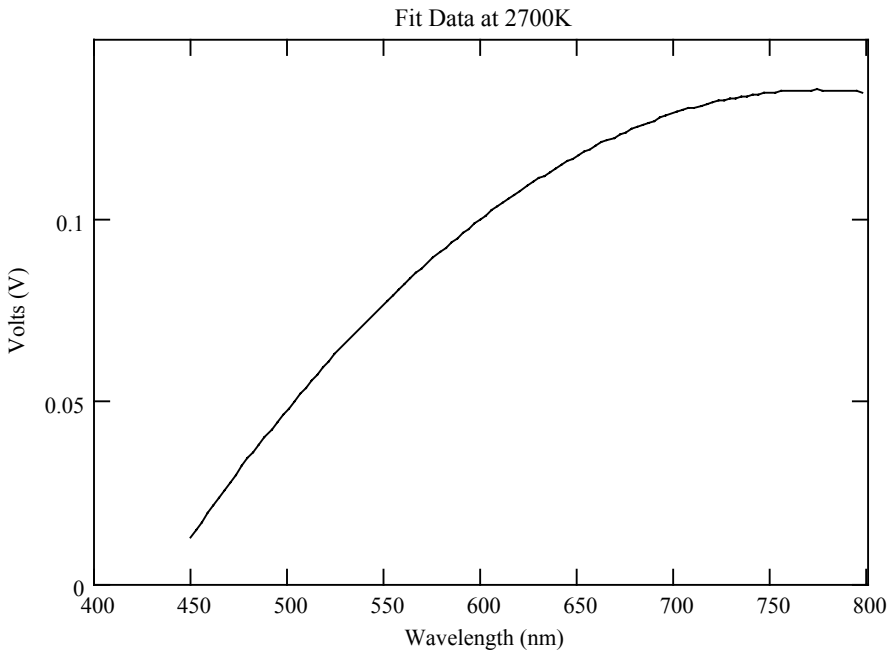

Figure B.8: Plot of curve fitted to data points

Once data table is updated all equations are recalculated and new plots are automatically generated, making it possible to analyze the results immediately.

APPENDIX C

ADVANTECH PCL CARD

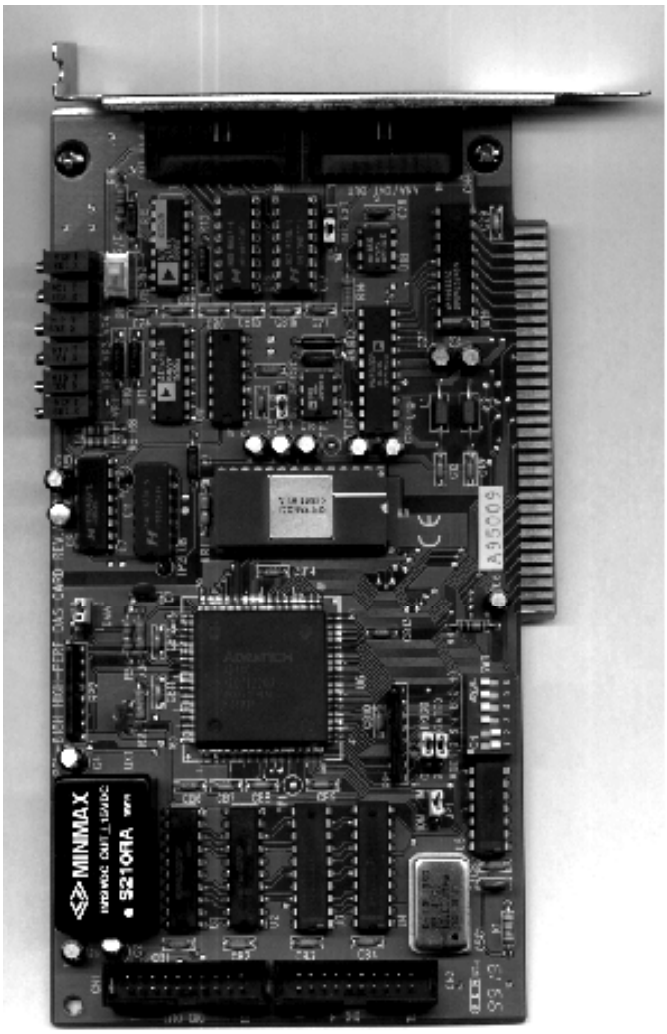

Figure C.1: Advantech PCL818 ADC card

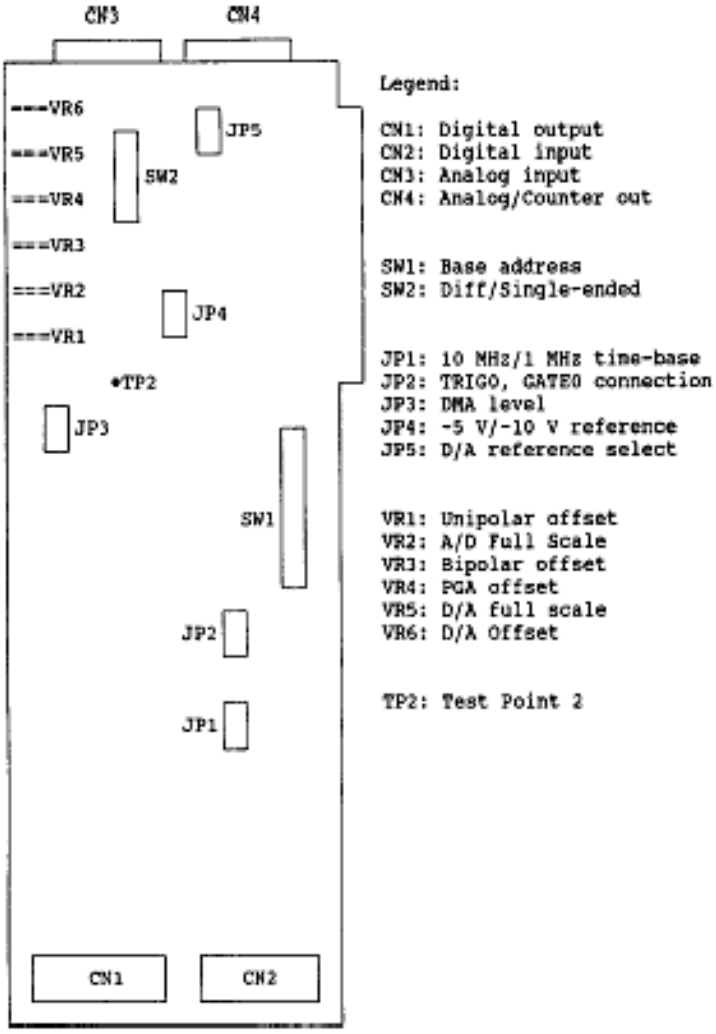

Figure C.2: PCL 818 Switch and jumper locations